UPPSALA
UNIVERSITET

Digital Comprehensive Summaries of Uppsala Dissertations from the Faculty of Science and Technology 1438

Inter-annual variability of rainfall in Central America

Connection with global and regional climate modulators

TITO MALDONADO

ACTA
UNIVERSITATIS
UPSALIENSIS
UPPSALA
2016

ISSN 1651-6214
ISBN 978-91-554-9716-3
urn:nbn:se:uu:diva-304656

Dissertation presented at Uppsala University to be publicly examined in Axel Hambergsalen, Villavägen 16, Uppsala, Friday, 25 November 2016 at 10:00 for the degree of Doctor of Philosophy. The examination will be conducted in English. Faculty examiner: Professor Michael Taylor (Department of Physics Faculty of Pure and Applied Sciences, Mona Campus, University of the West Indies.).

Abstract

Maldonado, T. 2016. Inter-annual variability of rainfall in Central America. Connection with global and regional climate modulators. *Digital Comprehensive Summaries of Uppsala Dissertations from the Faculty of Science and Technology* 1438. 67 pp. Uppsala: Acta Universitatis Upsaliensis. ISBN 978-91-554-9716-3.

Central America is a region regularly affected by natural disasters, with most of them having a hydro-meteorological origin. Therefore, the understanding of annual changes of precipitation upon the region is relevant for planning and mitigation of natural disasters. This thesis focuses on studying the precipitation variability at annual scales in Central America within the framework of the Swedish Centre for Natural Disaster Science. The aims of this thesis are: i) to establish the main climate variability sources during the boreal winter, spring and summer by using different statistical techniques, and ii) to study the connection of sea surface temperature anomalies of the neighbouring oceans with extreme precipitation events in the region.

Composites analysis is used to establish the variability sources during winter. Canonical correlation analysis is employed to explore the connection between the SST anomalies and extreme rainfall events during May-June and August-October. In addition, a global circulation model is used to replicate the results found with canonical correlation analysis, but also to study the relationship between the Caribbean Sea surface temperature and the Caribbean low-level jet.

The results show that during winter both El Niño Southern Oscillation and the Pacific Decadal Oscillation, are associated with changes of the sea level pressure near the North Atlantic Subtropical High and the Aleutian low. In addition, the El Niño Southern Oscillation signal is intensified (destroyed) when El Niño and the Pacific Decadal Oscillation have the same (opposite) sign.

Sea surface temperature anomalies have been related to changes in both the amount and temporal distribution of rainfall. Precipitation anomalies during May-June are associated with sea surface temperature anomalies over the Tropical North Atlantic region. Whereas, precipitation anomalies during August-September-October are associated with the sea surface temperature anomalies contrast between the Pacific Ocean and the Tropical North Atlantic region. Model outputs show no association between sea surface temperature gradients and the Caribbean low-level jet intensification. Canonical correlation analysis shows potential for prediction of extreme precipitation events, however, forecast validation shows that socio-economic variables must be included for more comprehensive natural disaster assessments.

Keywords: Precipitation, climate variability, El Niño Southern Oscillation, Tropical North Atlantic, Canonical Correlation Analysis, EC-EARTH, Caribbean Low-Level Jet

Tito Maldonado, Department of Earth Sciences, LUVAL, Villav. 16, Uppsala University, SE-75236 Uppsala, Sweden.

ISSN 1651-6214
ISBN 978-91-554-9716-3
urn:nbn:se:uu:diva-304656 (http://urn.kb.se/resolve?urn=urn:nbn:se:uu:diva-304656)

Sammanfattning

Centralamerika är en region som regelbundet drabbas av naturkatastrofer, de flesta av dem med hydro-meteorologiskt ursprung. Att förstå av nederbördens årliga variationer är centralt för planering och för att kunna begränsa omfattningen av naturkatastrofer i området. Denna avhandling fokuserar på nederbördens årliga variationer i Centralamerika och är gjord inom ramen för nationellt centrum för forskning i naturkatastrofslära (Centre for Natural Disaster Science, CNDS). Syftet med avhandlingen är: i) att etablera de viktigaste faktorer som styr klimatvariationer under vintern, våren och sommaren genom att använda olika statistiska metoder, och ii) att studera relationen mellan havsytans temperatur (Sea Surface Temperature, SST) och extrem nederbörd i regionen.

Statistiska metoder tillampas för att bestämma orsäker till variabilitet under vintern samt sambandet mellan SST och extrema regnhändelser under maj-juni och augusti-oktober. Dessutom, används en global klimatmodell för att reproducera resultaten från de statistiska metoderna och för att studera relationen mellan yttertemperatur i Karibiska havet och den Karibiska vindmaximat (Caribbean Low Level Jet, CLLJ).

Under vintern är global circulations mönster, både El Niño Southern Oscillation (ENSO) och den Pacific Decadal Oscillationen (PDO), förknippade med variationer av atmosfärens tryck vid havsytan nära Nordatlantiska subtropiska högtrycket och det Aleutiska lågtrycket. ENSO signalen intensifieras (dämpas) när El Niño och PDO har samma (motsatt) tecken.

Anomalier i ytvatten temperaturen kan förklara förändringar i både mängden och fördelning av regn över tid. Nederbördsanomalier under maj-juni är förknippade med havsytans temperaturavvikelser över den tropiska nordatlantiska regionen. Nederbörds avvikelser under augusti-september-oktober förklaras av kontrasten mellan havsytans temperaturavvikelser i Stilla havet och den tropiska nordatlantiska regionen. Modellresultaten visar inget samband mellan vattenytan temperaturgradienter och intensifiering av CLLJ. Statistiska metoder har utvecklats för att kunna prognostisera extrem nederbörd, dessa behöver ytterligare validering och att inkludera socioekonomiska variabler för att kunna göra mer omfattande bedömningar av riskerna för naturkatastrofer.

List of papers

This thesis is based on the following papers, which are referred to in the text by their Roman numerals.

I. Maldonado, T., A. Rutgersson, J. Amador, E. Alfaro, and B. Claremar, 2016: Variability of the Caribbean low-level jet during boreal winter: large-scale forcings. *International Journal of Climatology*, **36(4)**, 1954-1969, doi:10.1002/joc.4472.

II. Maldonado, T., A. Rutgersson, E. Alfaro, J. Amador, and B. Claremar, 2016: Interannual variability of the midsummer drought in Central America and the connection with sea surface temperatures, *Advances in Geosciences*, **42**, 35-50, doi:10.5194/adgeo-42-35-2016.

III. Maldonado, T., A. Rutgersson, R. Caballero, F. S. R. Pausata, E. Alfaro, and J. A. Amador, 2016: The Role of the Meridional Sea Surface Temperature Gradients in Controlling the Caribbean Low-Level Jet. *In Review*.

IV. Maldonado, T., E. Alfaro, A. Rutgersson, and J. Amador, 2016: The Early Rainy Season in Central America: the Role of the Tropical North Atlantic SSTs. *In Review*.

V. Maldonado, T., E. Alfaro, B. Fallas-López, and L. Alvarado, 2013: Seasonal prediction of extreme precipitation events and frequency of rainy days over Costa Rica, Central America, using Canonical Correlation Analysis. *Advances in Geosciences*, **33**, 41-52, doi:10.5194/adgeo-33-41-2013.

Reprints were made with permission from the publishers.

In Paper I, II, and III the author was the scientific coordinator. The author also had the main responsibility for analyzing the data and writing the main text. In Paper IV and V the author shared the scientific coordination, however, the author was the person in charge of the manuscript production.

Contents

1. Introduction

1.1 Central America and the Study of Natural Disasters

Central America is a region regularly affected by natural disasters. The categorization of these catastrophes covers a vast variety of natural hazards, due to its geographic location, prolonged cyclonic seasonality from both the Caribbean Sea and Pacific Ocean, geomorphology, and threats with hydro-meteorological origin. This region has a persistent occurrence of isolated phenomena or in combination amongst them, generating physical damage and economical losses, due to intense events (less frequent), but also to a large number of high frequency meteorological events of low intensity, being the impacts with climatic origin the most reported disasters (Wahlstrom, 2014). In fact, Retana (2012) found that the indirect effect of hurricanes over Central America, causes more precipitation, with higher occurrences from September to November, and major impact over the Pacific slope. Cold surges were identified as a secondary mechanism of rainfall production (Retana, 2012; Alfaro and Pérez-Briceño, 2014), affecting mainly the north and Caribbean sides of Costa Rica from December to January. Retana (2012) reported low pressure systems occur between April to November, however their effects are more homogeneous over the region.

Natural disasters, however, depend on the degree of vulnerability of the exposed elements, rather than the phenomenon's occurrence (Muñoz et al., 2012; Neri and Magaña, 2016). Alfaro et al. (2010) found that the recent increment of annual impact reports due to hydro-meteorological events cannot be explained using only the climatic effects, being necessarily to include socio-economic variables. In addition, the complex topography of the region makes that the study of climatic effects must require a regional approach. The typical spatial resolution of global models ($\sim$ 100 km) does not represent adequately the land-use nor the orographic features of the region (Amador and Alfaro, 2009; Oglesby et al., 2016). Dynamical and statistical downscaling are the common approaches often used to downscale the information from global models (known as General Circulation Models, GCM) to regional scales (Amador and Alfaro, 2009).

The Centre for Natural Disaster Science (CNDS) is a Swedish center for interdisciplinary research on natural hazards and disasters. The investigations conducted at CNDS aim to contribute to society by improving the ability to prevent and deal with risks associated to natural hazards by raising awareness of the dynamics and consequences of them. Within the CNDS framework, the present thesis examines climatic modulators of precipitation and their impact over Central America. The present work also provides tools for both studying and forecasting the seasonal rainfall in Central America.

2. Background

Central America and the Caribbean regions are home of about eighty million of people. Formed by countries and islands among the poorest of the Americas and even of the world, many of their inhabitants are living in areas prone to natural disasters. Alfaro et al. (2010) pointed out that most of the natural disaster reports have been related to hydro-meteorological phenomena. Indeed, this region is constantly affected by a wide variety of intense meteorological events, like traveling easterly waves, tropical cyclones, convective systems, cold surges coming from the northern hemisphere, the mid-summer drought (in Spanish *canícula or veranillo*), the warm pools, the trades, and an intense low-level jet over the Caribbean Sea. Variations in the intensity of these elements in combination with social factors (i.e. people living in risky areas), can increase the probability of natural disasters (Retana, 2012; Alfaro and Pérez-Briceño, 2014; Wahlstrom, 2014).

The understanding of the annual and seasonal precipitation cycle and its variation through the year, thereby, becomes essential for planning and preparation for the rainy season. The annual rainfall cycle in Central America is known to have two contrasting regimes between the Caribbean and Pacific slopes, due mainly to the interaction of the trades winds with the complex topography in the region. While in the Pacific side a semi annual feature is observed through the year, with the first rainfall maximum occurring during May-June, and a secondary and more intense peak in August to October, the Caribbean side exhibits wetter and more humid conditions during the winter months, concomitant to a precipitation minimum in the Pacific slope. The reduction in precipitation during July is due to different processes compared to those at the beginning of the year. Therefore, this relative decrease is a relevant element to explain the annual rainfall cycle. This reduction in rainfall has been called the mid-summer drought (MSD). Furthermore, almost simultaneously with the dry periods and the MSD in the Pacific slope (e.g. Magaña et al. 1999), a strong low-level wind current known as the Caribbean low-level jet (CLLJ) occurs twice per year. Both elements remain as a scientific challenge since little is known about their origins and interactions with other climate processes in the region (Amador, 2008).

The precipitation regime in Central America is highly modulated by the interaction of several climate processes that occur every year, that range from local and regional scales such as those mentioned above, to large scales forcing such as El Niño Southern Oscillation (ENSO), the Pacific Decadal Oscillation (PDO), and the North Atlantic Oscillation (NAO). ENSO, however, is the main climate modulator during both winter and summer in the region (Hidalgo et al., 2015). ENSO signal, nevertheless, is known to show inherent variability at high and mid latitudes, that in certain cases has been associated to non-linearities, and in other cases to the interaction with the PDO.

At regional scales, previous studies have analyzed the influence of the sea surface temperature (SST) anomalies in the precipitation regime in Central America. Enfield and Alfaro (1999) have shown that the magnitude of the precipitation during the rainy season (from May to October) in Central America is highly modulated by the SST anomalies at both oceans, the Pacific and the Atlantic. Alfaro (2007b) and Fallas-López and Alfaro (2012a) studied the predictability of the rainfall using canonical correlation analysis (CCA) with SST as predictor. Both studies found that the SST modify the response on precipitation in different ways during each rainfall maximum, the first rainfall peak being modulated mainly by the SST over the tropical Atlantic, and the secondary maximum being controlled by a dipole in the SST anomalies over the neighboring oceans to the Central American coast. Moreover, Fallas-López and Alfaro (2012b) found that the MSD intensity is dependent on several global climate indexes such as the Atlantic Multi-Decadal Oscillation (AMO), Niño 3 (N3), and PDO. Maldonado and Alfaro (2011) and Paper V utilized Canonical Correlation Analysis CCA to explore the distribution of precipitation extreme events during the second precipitation maximum, finding that during the second rainfall maximum, the total precipitation and temporal distribution of precipitation events are controlled by a dipole in the SSTs between the Pacific and the Caribbean-North Atlantic waters. Given the above evidence, it would be expected that the SST is involved in the MSD variability at inter-annual scales. In fact, Alfaro (2014) found that warm (cool) conditions of Niño 3.4 tend to be associated to drier (wetter) MSD events in some regions of the North Pacific and the Central Valley of Costa Rica.

2.1 Aims of study

According to Wahlstrom (2014) the impact of high frequency meteorological events represent the majority of economic and human losses. Precipitation, in the other hand shows high spatial and inter-annual variability, thus, the prediction of precipitation anomalies in the region is a difficult task. Therefore, the aim of this thesis is to study the inter-annual variability of precipitation in Central America, and its connection to global and regional climatic modulators. The framework of this study also proposes a systematic methodology for seasonal precipitation forecasting in the region. To achieve this goal, the study has been subdivided into specific objectives due to the marked rainfall seasonality:

- Studying the variability of El Niño and PDO and its impact on precipitation during boreal winter.

- To explore the relationship of heavy rainfall events in May-June and their connection with the Tropical North Atlantic sea surface temperatures.

- To analyze the inter-annual variability of the mid-summer drought and its relationship with the sea surface temperatures of neighboring oceans.

- Studying the relationship between the meridional sea surface temperature gradient over the Caribbean Sea, Caribbean low-level jet and precipitation in Central America.

- To explore the potential of Canonical Correlation Analysis for forecasting precipitation during the rainy season, using sea surface temperatures anomalies as predictor.

The scientific papers presented in this thesis relate to all of these objectives. The most relevant results are summarized and discussed in this document, in the context of natural disasters. This thesis contributes to the current knowledge about the weather and climate dynamics in the Central American region. In practical terms, the results of this thesis will contribute to the improvement of the design, planning and implementation of warning and mitigation strategies oriented to the assessment of severe dry conditions, like the droughts reported in the North Pacific region of Costa Rica during July 2014 (Chinchilla-Ramírez, 2014). The results will improve the pool of information currently available to both social and economical sectors, such as emergency offices, water resources, agricultural and hydro-electrical power production parties among others, contributing to a better response to eventual emergency situations linked hydrological events in winter and summer periods.

3. Climatic Features

The geographical location of Central America plays a significant role to describe the climate and the variability of the region. Surrounded by two large water masses, the Eastern Tropical Pacific (ETPac) ocean at the western side (Fiedler and Lavín, 2006), and the Caribbean Sea at the eastern side; along with the Gulf of Mexico, the entire area is known as the Intra-Americas Sea (IAS, Amador 2008) as shown in Fig. 3.1. The IAS is also important for the global climate, because it receives large amounts of radiation coming from the Sun onto the Earth surface, and the regional waters act like an energy reservoir.

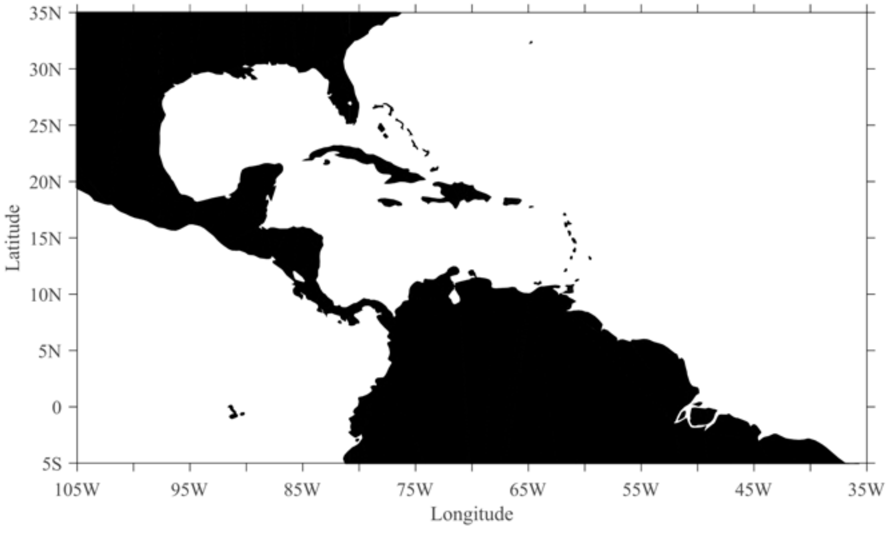

Figure 3.1. The Intra-Americas Sea (IAS) region.

The IAS region is sensitive to the effect of both large- and regional-scale dynamical systems acting in its vicinity, such as the North Atlantic Subtropical High (NASH), strong easterly winds, a large latent heat belt, warm sea surface temperature SST and intense precipitation. All of these elements depict the general frame of the regional climate and variability in the region (Wang et al., 2008). Furthermore, the formation of the Western Hemisphere Warm Pool (WHWP, Wang and Enfield 2001, 2003; Wang and Fiedler 2006), cyclogenesis over the Caribbean Sea (Goldenberg et al., 2001), the influence of the Inter Tropical Convergence Zone (ITCZ) along with the MSD (Magaña et al. 1999; Karnauskas et al. 2013; Herrera et al. 2015, Paper II), and the

CLLJ (Amador 1998, 2008, Paper III) form part of the vast variety of regional climate components present in this area. Many of the dynamical and physical mechanisms and interactions with the climate of the region are still not fully understood (Amador, 2008).

3.1 The Wind Field

The trade winds are the low-level tropospheric flow, classically known as part of the equator-ward branch of the Hadley cell transporting a large amount of the moisture, resulting in convergence with uplift and destabilized stratification at the low latitudes. They are responsible for the convective activity and associated precipitation distribution that take place near or within the ITCZ. At local scales, the interaction with the topography helps to explain the temporal and spatial rainfall variability in some areas of Central America (Amador et al., 2003). Two subtropical high-pressure systems located near 30° N, in both the Pacific Ocean (the North Pacific High) and in the North Atlantic Ocean (the Bermuda or Azores High), produce, in average, a relative strong meridional pressure gradient between the subtropics and tropics, which accelerates the air masses towards the equator, generating the trade winds.

Monsoonal systems such as the North American Monsoon System (NAMS) and the South American Monsoon System (SAMS) interact in different ways with the trade winds, and are important mechanisms to explain the precipitation during the warm season in the ETPac. Vera et al. (2006) review both systems with more details. According to Amador et al. (2006), the most relevant for ocean-atmosphere dynamics in the ETPac is the NAMS.

During the northern hemisphere winter, the ITCZ is at its southernmost position (Srinivasan and Smith, 1996), and SSTs over the adjacent areas of the Caribbean and the Pacific are relatively uniform, with values usually below 28 °C (Amador et al., 2003). Trade winds are intensified and a frequent southward displacement of air masses occurs. From December – March cold air masses coming from Canada and the polar regions penetrate deep into the tropics and produce strong wind events associated with intense periods of rainfall (Schultz et al., 1997, 1998; Zárate-Hernández, 2013). Interaction with topography (i.e. wind is funnelled trough topographical gaps in southern Mexico and Central America), and a strong gradient in the sea level pressure (SLP) between the basins, a low in the Pacific and a high in the Caribbean, due to the intrusion of cold outbreaks, produce strong near-surface wind events that can extend far in the ETPac (Amador et al., 2006; Alfaro and Cortéz, 2012). High SLP over the southwester Caribbean generates northerly surface winds across the Isthmus of Panama that extend offshore of the Gulf of Panama into the eastern tropical Pacific region (Amador et al., 2006). During this season these intense winds over the Caribbean are associated with the winter branch of the

CLLJ (Wang and Lee 2007; Amador 2008, Paper I), and its interaction with mountains forces rainfall in Central America.

In the boreal summer, more complex circulations than those in winter develop in the IAS region. The NAMS is generated due to the seasonal thermal contrast that occurs in this season over the ETPac, and the North, Central and South America masses (e.g. Higgins et al. 2003). The NAMS has been shown to be associated with the summertime precipitation of the region (Mock, 1996; Higgins et al., 1997). It starts to develop during May – June, and associated with heavy rainfall in late May or early June over southern Mexico, moving north to the south-western United States. The mature phase is reached during July – August and September, and the precipitation regime over North America is related to NAMS (Higgins et al., 1997). Surges of maritime tropical air that move northward are associated with rainfall over the Gulf of California and southwester United States (Douglas and Leal, 2003). The decay phase (late September – October) can be characterized as broadly the reverse of the onset phase, though at a slower rate (Higgins et al., 2003).

Other low-level flows occur during the boreal summer, particularly the Gulf of California low-level jet (Douglas, 1995; Douglas et al., 1998), the Chocó low-level jet (Poveda and Mesa, 2000), and the Caribbean low-level jet (Amador, 1998, 2008). The former is parallel to the Gulf axis and has a well defined diurnal and synoptic scale variability. It is located below 2000 m at the northern end of the Gulf of California with wind velocities of $5-7\mathrm{ms}^{-1}$. It is a relevant mechanism for moisture transport into the interior of the continental regions during the monsoon (Douglas and Leal, 2003).

The second mechanism, the Chocó jet (CJ) develops in the western coast of Colombia near 5° N. It reaches its maximum by October-November, then decreases its intensity until being almost absent during the period February-March. Low-level warm air and moisture convergence associated with the CJ, low surface pressure and orographic vertical motion on the western Andes, contribute to deep convective activity, which is organized as meso-scale convective complexes.

The third low-level flow, the CLLJ, peaks in both winter and summer (Amador 1998; Amador et al. 2003; Amador 2008, Paper III). The mean annual cycle of the CLLJ index at 925 hPa is shown in Fig. 3.2. During summer, it is barotropically unstable, and has potential interaction with transients, such as easterly waves. From May to July, easterly waves loose energy and momentum strengthening the mean current and causing the low-level jet to peak in July. The CLLJ is an important element to explain the convective activity during July through November, and contributes to understand the climate of the region. In winter, however, its formation is distinct to the summer component (Amador 2008; Wang 2007; Cook and Vizy 2010, Paper I), nevertheless, it is an important mechanism for moisture transport from the Caribbean Sea to Central America and the Gulf of Mexico during both seasons (Durán-Quesada et al., 2010; Gimeno et al., 2012).

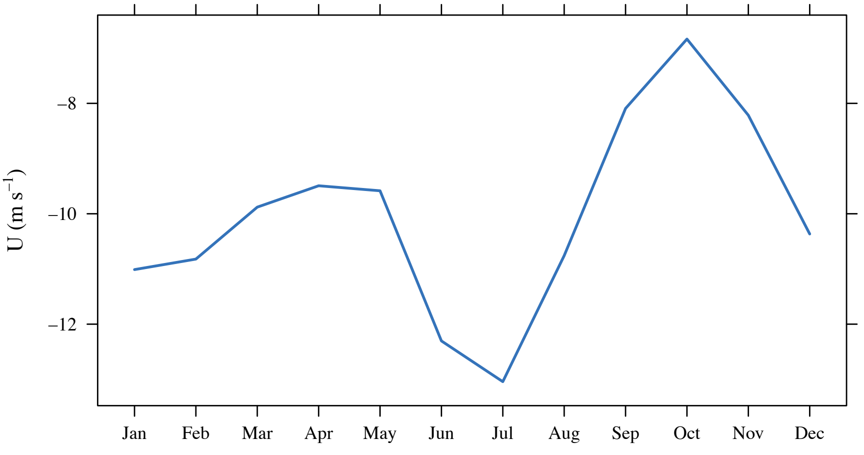

Figure 3.2. Mean annual cycle of the Caribbean low-level jet index in ms^{-1}. Note that since the wind is easterly, the more negative values mean stronger zonal wind (from Paper I).

According to Amador et al. (2006), the wind stress curl has a strong seasonal cycle with a marked meridional migration of the up-welling (positive curl) and down-welling (negative curl) areas that is mostly associated with the southeast and northeast trade patterns and its north-south migration in the eastern tropical Pacific. The distribution of this variable is almost zonal, and most of the large-scale features are located north of the equator. In general, the fluctuations in the magnitude of the wind stress curl in the tropics are mainly related to seasonal atmospheric circulation and the ITCZ.

3.2 Moisture Transport

Durán-Quesada et al. (2010) identified two main moisture sources for Central America. The first one and the most important is located in the Caribbean. The second appears to exist near the equatorial Pacific region. These results were highlighted also by Gimeno et al. (2012) whose stress that the major amount of humidity in the Continental part of Central America is originated in the nearby oceans. A third continental source of moisture was found by Durán-Quesada (2012) over Venezuela due to water recycling processes.

The intensity and extent of the moisture sources vary throughout the year. The Caribbean source (CS) does not vary significantly along the year, except by a slight displacement towards the Gulf of Mexico during winter. In contrast, the Pacific source (PS) shows significant variation throughout the year, and disappears as a source during winter and spring, mainly due to the influence of the ITCZ (Durán-Quesada et al., 2010). Seasonally, during the boreal summer the humidity transport from the CS is more effective and contributes with the precipitation in Central America, while the moisture that departs from PS is not even able to reach the entire Central America region, contributing only to precipitation in its southernmost portion, specifically at Costa Rica. Through the boreal winter, there is a reduction in the moisture transport, consistent with the precipitation pattern over this region, exhibiting dry conditions (mainly in the Pacific basin) during this season. Moisture convergence in Central America during winter is clearly less important than during spring (March, April, May) and autumn (September, October, November), when the moisture flux over the continental area of Central America becomes more relevant.

In order to understand the role of the CLLJ for moisture transport, it is worth to say that the CLLJ acts not only as a moisture belt, but also as a humidity collector that is capable of modulating surface evaporation as a result of its moisture content (Wang et al., 2007). Many studies found that the core of the CLLJ is consistent with the maximum nucleus of moisture gain over the Caribbean Sea (Wang, 2007; Wang and Lee, 2007; Wang et al., 2007; Durán-Quesada et al., 2010). The major contribution occurs during boreal summer, and for the case of the CS region this is in good agreement with the maximum observed winds in the core of the CLLJ. However, the second maximum of the CLLJ in boreal winter is not associated with any important transport, mainly due to the incidence of the dry season, which is characterized by less intense jet winds than in summer and a minimal amount of precipitable water.

Durán-Quesada et al. (2010) highlight that the contribution of moisture to Central America that originates in the PS region is partly determined by the presence of the CJ, which in turn allows the development of deep convection in the region. This contribution is more noticeable over northern Colombia when it appears to be combined with the effect of orographic lifting as described by Poveda and Mesa (2000). The importance of the PS region is greatest during those parts of the boreal summer and autumn that coincide with the maximum velocities within the core of the CJ. A significant part of the moisture transported by this jet is unable to reach Central America completely, mainly as a result of the loss of moisture in the ITCZ and the presence of a mountain range in Costa Rica.

3.3 Precipitation

The most relevant synoptic influence present in the Caribbean and Central America area is the NASH. This subtropical high produces strong easterly trades winds towards the equator, being in Central America the dominant wind regime. The interaction between the trades and the topography, plus the location of the isthmus, imprint upon the region particular climate and weather features. This interaction produces two regional climates – Pacific and Caribbean (Taylor and Alfaro, 2005; Amador et al., 2006), nonetheless, the complex orography is capable to produce very local climate and weather patterns, noted mainly in the high variability observed in precipitation with respect to the altitude (Fernández et al., 1996; Amador et al., 2003).

The Pacific side presents a bimodal rainfall distribution around the year (Fig. 3.3, top panel). A first maximum occurs in May-June, due in part to the migration north of the ITCZ. However, the migration of the ITCZ neither explains the generalized deep convection during the rainy season over the whole region since the ITCZ is not found at latitudes 10° – 12° N (Alfaro 2000, Paper IV), nor explain the beginning and the ending of the rainy spells. Additionally to this migration, the SST of the neighbouring seas have warmed reaching about 29 °C, deep convection activity is developed along with a sub-tropical lower-tropospheric cyclonic circulation anomaly over the subtropics.

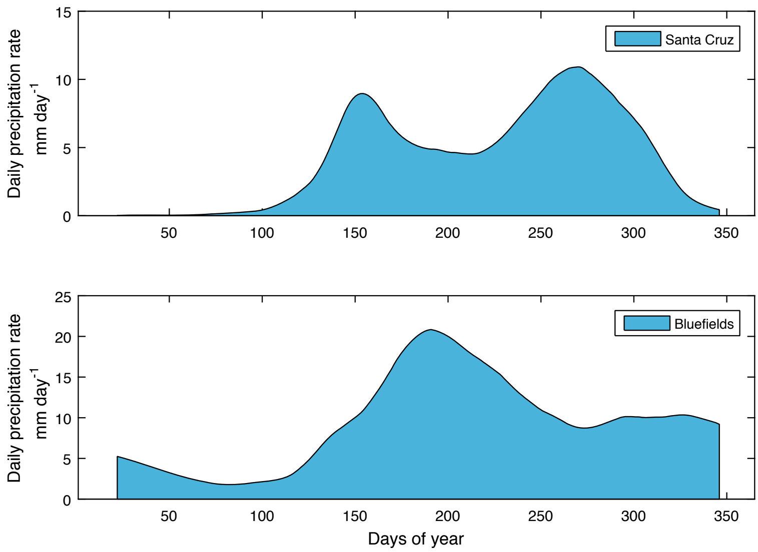

Figure 3.3. Examples of the mean precipitation annual cycle in the Pacific (top) and Caribbean (bottom) slopes.

A relative minimum of precipitation through July-August upon this slope, is due to the MSD (Magaña et al. 1999; Karnauskas et al. 2013; Herrera et al. 2015, Paper II). During the occurrence of the MSD in these months, the convective activity diminishes, due to a decrease of about 1 °C in the SST over the ETPac, the cyclonic circulation anomaly weakens, corresponding to an anticyclonic acceleration of the low-level flow and, therefore, to an intensification of the trade winds. This leads to a formation of divergence anomalies that inhibit deep convection activity, and the strengthening of the easterlies, forcing upward motion and intense precipitation over the Caribbean side, and subsidence and clear skies upon the Pacific slope (Hidalgo et al., 2015).

The second maximum peaks during August through October due to the presence of fewer deep clouds, which would produce an increment of incoming solar radiation increasing the SST above 28 °C. Then, this warming in the SST produces an increase of evaporation from the oceans to the atmosphere; in addition, weakened trade winds and a low-level convergence anomaly lead to enhanced deep convection. Normally, this season presents the highest frequency of extreme events over the Pacific slope (Alfaro et al. 2010, Paper V). While in the Caribbean side, rainfall decreases during these months, due to a decrease in the strength of the trade winds (Taylor and Alfaro, 2005; Amador et al., 2006). From December to March, the Pacific slope of Central America presents warm and mostly dry conditions. During these moths, the ITCZ is at its southernmost position (Srinivasan and Smith, 1996).

The Caribbean side shows (Fig. 3.3, bottom panel) a different rainfall mode, as pointed out by Taylor and Alfaro (2005). Precipitation during the winter months along this coast, is mostly related to humidity convergence, mid-latitude air intrusions (Schultz et al., 1997, 1998), and less frequent low-level cloud systems traveling from the east (Velásquez, 2000).

3.4 Variability elements in the Intra-Americas Sea

3.4.1 Large-scale variability modulators

ENSO is the most influential large scale index on the climate of the IAS (Wang and Fiedler, 2006). Nevertheless, the influence of other variability modes in the Atlantic Ocean such as the AMO, and the NAO have shown to have an important contribution in the variability of the precipitation field of Central America (Enfield and Alfaro 1999; Alfaro 2007b; among others). Recently, the influence of the PDO on rainfall over the Central America (Mantua and Hare 2002; Fallas-López and Alfaro 2012b, Paper I, IV, V), the influence of the Madden-Julian Oscillation (Martin and Schumacher, 2011; Poleo et al., 2014a,b) on precipitation in the Caribbean islands have also been studied.

El Niño Southern Oscillation

ENSO is a two-component physical mechanism that describes the coupling of SST anomalies in the tropical Pacific Ocean and the fluctuation in tropical SLP gradient in the Western and Eastern Pacific Hemispheres, also known as the Southern Oscillation. El Niño is associated with unusual strong warming events that occur every two to seven years in concert with basin-scale tropical Pacific anomalies (Wang and Fiedler, 2006). ENSO variability in the eastern tropical Pacific is centred along the equator, but is closely related to variability of the tropical WHWP. Authors such as Chen and Taylor (2002) and Bell and Chelliah (2006) suggest that ENSO forces variations in the SST field and vertical wind shear that trigger the inter-annual variability of the hurricane season during ENSO events. Moreover, an increase (decrease) of precipitation has been associated with cold (warm) ENSO phases (Dai and Wigley 2000; Giannini et al. 2000, Paper I).

Variability of the surface winds has also been observed related to ENSO. During summer, the flow over the surface has been found to increase during El Niño events while a reduction occurs in the opposite phase. Examples of that, are the changes in the CJ (Poveda and Mesa, 2000) and the CLLJ (Wang, 2007; Amador, 2008). The core intensity of the CLLJ varies with ENSO phases in such way that during warm (cold) events the jet core is stronger (weaker) than normal in the boreal summer, surface wind stress and wind stress curl area are expected to be stronger (weaker) than normal in the easternmost portion of the eastern tropical Pacific. Contrary to what happens in summers, the jet core is weaker (stronger) than normal during warm (cold) ENSO phases in winter (Amador 2008, Paper I). These variations in the wind field influence the vertical wind shear and cyclone-genetic processes (Amador, 2008; Amador et al., 2010).

ENSO events, therefore, are able to affect precipitation distribution by modulating two different mechanisms: a) evaporation variability linked to SST and surface drag variations and b) transport of moisture due to wind flow modulation.

The Pacific Decadal Oscillation

The PDO is a long-lived El Niño-like pattern of the variability of the Pacific climate (Zhang et al., 1997). Mantua et al. (1997) highlight the PDO as the dominant pattern of Pacific Decadal Variability. Even when the PDO is referred as an El Niño-like pattern, it differs from ENSO in the time scale of the persistence of events and its fingerprint is more noticeable in the extratropics rather than the tropics (Mantua and Hare, 2002). The pattern of a warm PDO phase is featured by cooler than normal SSTs in the central North Pacific and warmer than normal SSTs along the west coast of the Americas. Symmetry in SST anomalies patterns between northern and southern hemispheres exhibited by the PDO has been noted by Evans et al. (2001). The mechanisms of the PDO are complex and still an open issue, however, some studies suggest the importance of the tropical coupling for the existence of the PDO (Feng et al., 2010). Schneider and Cornuelle (2005), propose the PDO to evolve from a composition between the forcing due to Niño 3.4 (see Trenberth 1997 for definition of El Niño regions), and the changes of the Aleutian low (interannual frequencies) and the Kuroshio-Oyashio Extension (decadal time scales). The importance that the PDO may have for global climate is related to a correlation between the PDO index (Mantua et al., 1997) and precipitation anomalies. Warm PDO phases have been found associated with anomalously dry periods in the eastern coasts of Eurasia, Northwest Pacific of USA, Central America and northern South America. While the same phase seems to be related to wetter than normal conditions in the Gulf of Alaska, South-west USA and Mexico, South-east Brazil, South central South America and western Australia. In Paper I is found that during winter the PDO forcing is more appreciable in combination with the El Niño phases. The PDO intensifies El Niño signal in

SLP and precipitation anomalies, if both processes have the same phase. The PDO, however, modulates precipitation mainly over Mexico and southern part of USA.

The North Atlantic Oscillation

Greatbatch (2000) made a detailed revision of the NAO. It is the most important variability mode in the North Atlantic Ocean. One way to define and index for NAO is like the difference between normalized mean winter (December to March) SLP anomalies at Lisbon, Portugal and Stykkisholmur, Iceland (Hurrell, 1996). NAO is an element of the Arctic Oscillation pattern, then the former is linked with SST anomalies in the East/South-east of Greenland.

NAO has been also associated with the strengthen of the NASH and the North Eastern trade winds, affecting thus the circulation in the IAS. Thereby, the impact of the NAO is associated with climate features over the IAS, SST in the Tropical North Atlantic, the size of the WHWP and the CLLJ. Seasonal variations of the NAO may be reflected in its influence on the IAS easterly winds and precipitation patterns (Wang, 2007). Malmgren et al. (1998) found that during the boreal summer the NAO index has an inverse relation with the observed precipitation patterns over Puerto Rico.

The Atlantic Multi-Decadal Oscillation

The AMO is a 70 years period mode in SST (Delworth and Mann, 2000; Kerr, 2000). This signal has also been found in different modeling analysis (Delworth et al., 1993; Delworth and Greatbatch, 2000; Latif et al., 2004) and it was detected as the first rotated empirical orthogonal functions (EOF) with a large response in the North Atlantic SST (Mestas-Nuñez and Enfield, 2001). The AMO signal modulates precipitation variations in different regions such as the IAS (Giannini et al., 2000). Wetter (drier) conditions over Central America (north-east Brazil) during JJA (DJF) were found by Zhang and Delworth (2006). AMO has also been determined to be of importance modulating the impact of ENSO on droughts. The connection between AMO and other regional features such as the Atlantic Warm Pool (AWP) has been also studied. Wang et al. (2008) show that warm (cool) phases of the AMO are associated with repeated large (small) AWPs, suggesting the relationship between the AMO and Atlantic tropical cyclones. The latter is in agreement with results that indicate the presence of multi-decadal variations in hurricane activity due to the Atlantic SST (Goldenberg et al., 2001). AMO is then of importance related to the low frequency variability of precipitation as it modulates the distribution of moisture and extreme rainfall events (Paper V).

3.4.2 Regional-scale Modulators

Regional circulations Systems

Two important regional circulation systems modulate the weather and climate in the region. The first mechanism is the CLLJ over the Caribbean Sea, and the second the Chocó LLJ.

The CLLJ is important for moisture transport in the region, and also to explain the convective activity during the summer months. During winter, it has a second maximum, nonetheless, it has shown no relation with convection during this season (Amador et al. 2006; Amador 2008, Paper I, III). The Chocó LLJ peaks in October-November, and contributes to the moisture transport for the southernmost part of Central America (Durán-Quesada et al., 2010). Furthermore, the Chocó jet is associated with deep convection activity over the western Andes region in Colombia (Poveda and Mesa, 2000).

SST of Neighboring Oceans

The influence of the SST anomalies on the precipitation variability field has been widely studied (Enfield and Alfaro, 1999; Alfaro, 2000, 2007b). The beginning and ending of the rain spells are related to fluctuations in the SST of the Atlantic and Pacific Oceans. SST anomalies are also associated with the magnitude of rainfall and frequency of rainy days (Maldonado and Alfaro 2010a, 2011, Paper V). Amador et al. (2006) pointed out that the seasonal cycle of SST is important in defining key climatological features, especially during summer-autumn, such as the WHWP development (Wang and Enfield, 2001; Wang and Fiedler, 2006), the appearance of MSD (Magaña et al. 1999; Karnauskas et al. 2013; Herrera et al. 2015, Paper II), and favorable areas for cyclogenesis (Goldenberg et al., 2001). During the northern winter, SST isotherms over the Caribbean and the eastern tropical Pacific are mostly zonally distributed, with values usually below 28 – 29 °C, except in the central eastern tropical Pacific, and to the west of Central America, where there is a maximum of SST throughout the year. As result of this SST distribution, there is a relatively strong vertical trade wind shear, along with a reduction in evaporation. These conditions do not allow major convective activity to occur in most of the Pacific slope of Central America during this season. In addtion, the ITCZ is at its southernmost position (Srinivasan and Smith, 1996) during the boreal winter.

In boreal summer, the WHWP dominates the SST distribution over most of the eastern tropical Pacific region (Magaña et al., 1999; Wang and Enfield, 2001, 2003). In the Caribbean warm pool, organized activity is barely observed, due mainly to a strong vertical wind shear and strong subsidence associated with regional scale circulations, such as those associated with the CLLJ. During warm (cold) ENSO phases, the CLLJ shows stronger (weaker) than normal wind speeds (Amador et al., 2003, 2006; Amador, 2008). This fluctuation is reflected in SST anomalies over the Caribbean Sea, north coast of Venezuela; a strong (weak) jet results in negative (positive) SST anomalies over this region due to strong (weak) Ekman transport. In this way, the jet may have a role in coupling SST anomalies in eastern Pacific during El Niño or La Niña events with anomalies over some regions of the Caribbean during summer. Variations in surface variables (precipitation and temperature) in different sectors of Mesoamerica, including its west coast, are the result of a combination of fluctuations in the equatorial tropical Pacific and in the tropical north Atlantic (Amador et al., 2006). Studies such as Alfaro et al. (1998); Alfaro and Cid (1999a,b); Enfield and Alfaro (1999) show that the strongest rainfall signal occurs when tropical north Atlantic and tropical Pacific SST anomalies are in a configuration of meridional dipole (antisymmetric) across the ITCZ, that is, when this anomalies have an opposite sign. The rainy season in south Central America tends to start early and end late in years that begin with warm SST in the tropical North Atlantic. Ending dates are also delayed when the eastern tropical Pacific is cold.

The influence of regional meridional SST gradients on the climate over the region has been already explored. Uribe-Alcántara (2002) found that the distribution of the SST is manifested along the rainfall season over the southwester coast of México. Furthermore, he proposed that the MSD is a consequence of the reduction of the meridional SST gradient upon the equatorial eastern Pacific due to the interaction between the ITCZ and the ocean. In the Caribbean the meridional SST gradient has a relevant connection with the CLLJ (Wang, 2007; Amador, 2008), as coupling mechanism between the sea and the atmospheric boundary layer. The latitudinal SST gradient over the Caribbean sea has been also proposed to be the main forcing in the intesification of the wind, that generates the CLLJ (Wang, 2007). The coupling between the CLLJ and the sea in this area is of relevance for both regional scales, due to the possible connection with the MSD (Herrera et al., 2015), and for global scales owed to the influence of the CLLJ on inter-annual variability of oceanic currents present over the Caribbean Sea (Chang and Oey, 2013). The interaction between the CLLJ and the meridional SST gradients, and its impact on the climate in Central America is studied in Paper III.

3.4.3 Local-scale Modulators

Topography is the main local modulator of the variability in the region. Interaction between the terrain with the induced flow coming from the Pacific ITCZ, due to some prevailing synoptic system, produces a type of disturbance that contributes to precipitation in Central America, which is named the "temporales" (Hanstenrath, 1991; Fernández et al., 1996). These are periods of weak-moderate nearly continuous rain, lasting several days and affecting a relatively large region. Their definition includes the condition that the wind must be weak; however, Amador et al. (2003) have shown that in some cases winds can be intense and long-lasting.

Fernández et al. (1996) identify at least four synoptic configurations that can eventually generate conditions for a temporal, such as a deep lower and middle troposphere troughs in the easterlies (hurricanes excluded), intrusions of an upper troposphere troughs in mid-latitude westerlies, outbreaks of cold air from North America (Zárate-Hernández, 2013), and the direct and indirect effect of hurricanes. Velásquez (2000) also found that westward- traveling, low-level cloud systems (Peña and Douglas, 2002) over the Caribbean reaching the Pacific, which are not necessarily associated with mid-latitude cold air intrusions. The frequency of these events presents a great deal of interannual and intraseasonal variability, and their relationship to ENSO or to other large-scale climatic signals is still unclear (Amador et al., 2006).

The sea-breeze circulations are other relevant regional modulators of the climate, on islands and peninsulas since they favors the development of convective systems. These circulations are marked by a diurnal cycle due to the thermal contrast between the coastline and sea. They can be associated to a diurnal cycle of precipitation. However, in coastal regions with nearby complex topography, like Central America, the induced flow can impact the temporal and spatial distribution of the meso-scale features in rainfall. Besides that, there is evidence in regions with similar characteristics to the Central American isthmus (i.e. west coast of Colombia), that the sea breeze can penetrate over near-coastal mountains into a valley until approximately 100 km (Warner et al., 2003). Nevertheless, note that such a feature of the sea breeze circulation has not been reported in Central America yet, but it might be a local modulator on many regions of this area.

4. Data

4.1 Area of Study

The area of study covers a large region, which has been divided into two domains in order to analyze processes at different scales. In order to capture the most important large-scale climate modulators for the region (see Section 3.4), the domain bounded by 22° S to 63° N and 111° E to 15° E is selected, covering basically all of the Pacific and Atlantic oceans. This domain is used in Paper I, II, IV and V. Regional-scale climate features are investigated using the domain 5° N to 35° N and 110° W to 40° W. The second domain is mostly used in Paper III and IV.

4.2 Reanalysis Data

In Paper I, data from the National Centers for Environmental Prediction – National Center for Atmospheric Research (NCEP-NCAR) reanalysis project (Kalnay et al., 1996) are used. This dataset has previously been utilized for climate studies in the region of study (e.g. Amador 2008; Herrera et al. 2015) and its time series are long enough to capture long-lived events such as the PDO. The NCEP-NCAR reanalysis has a spectral resolution T62 L28. The products are interpolated to a Gaussian grid of $2.5^\circ \times 2.5^\circ$ and 28 pressure levels. In Paper I the period 1950 – 2010 is taken for the SLP and horizontal wind fields. Although the NCEP-NCAR reanalysis has previously displayed deficiencies in its representation of precipitation in the tropics, mainly at regional scales, large-scale and inter-annual variability features are rendered in good agreement with observations (Janowiak et al., 1998). On the other hand, Janowiak et al. also pointed out that reanalysis fields such as wind, geopotential height, and temperature contained proper estimates of the observed values. Herrera et al. (2015) also pointed out that this reanalysis can capture important climate features in Central America, such as the MSD.

In Paper III and IV regional processes are studied. Therefore, ERA-Interim reanalysis (Dee et al., 2011) is used. This dataset has a finer spectral resolution type $T_L255L60$. The products are interpolated to a Gaussian grid of about $0.7^\circ \times 0.7^\circ$ and 60 pressure levels. The time series length is shorter than NCEP-NCAR reanalysis, starting on January 1979 to present. In Paper III the time length is cut to 15-years covering from 1990 to 2004, whereas in Paper IV the time length is 34 years from 1979 to 2012.

4.3 Precipitation Data

Monthly total precipitation estimates are obtained from the Global Precipitation Climatology Centre (GPCC, Schneider et al. 2011). The GPCC data are gridded with a 0.5° horizontal resolution. The dataset comprises monitoring products based on quality-controlled gauge station data from 1901 to the present. In Paper I, the climatology is estimated for the 1950 – 2010 period.

A total of 122 gauge stations, with daily observations of precipitation, are used. These measurements are provided by the meteorological services in Central America. In Paper II the number of stations is decreased to 25, owed to their better quality to represent the MSD in July-August, and the period start from 1961 to 2012. In Paper IV the complete set of stations are used, and the period of observations is from 1968 to 2012. The geographical location of the complete set of stations is shown in Fig. 4.1. In Paper V, a small of group of 29 stations, mostly located over Costa Rica, was used to produce and validate CCA forecasts against meteorological observations and natural disasters reports during the season August-September-October 2010. The period of this group of station covers from 1968 to 2008.

The gaps in the time series are filled using the methodology described in Alfaro and Soley (2009), which uses autoregressive models of order 1. This method can filter persistent signals comparable to the length of the filter and EOFs, and the estimated values are consistent with the statistical properties of the time series without external superposition of the data.

4.4 Sea Surface Temperature Dataset

The extended reconstructed sea surface temperatures (ERSSTv3b, Xue et al. 2003; Smith et al. 2007) are used in Paper II and IV. The SST anomalies are constructed using a combination of observed data along with models and historical sampling grids. This global database has a horizontal resolution of 2 by 2 degrees. The domain bounded by 22° S to 63° N and 111° E to 15° E. This domain has a complete representation of both oceans: the Pacific and Atlantic. The SST anomalies are used as predictors for the canonical correlation analysis method.

4.5 El Niño Southern Oscillation Events Definition

The ENSO episodes were determined using the definition of the Oceanic Niño Index (ONI)[1] from the NOAA's Climate Prediction Center (CPC). The ONI definition of warm (cold) events consists of a threshold of ±0.5 °C for the

[1] `http://www.cpc.ncep.noaa.gov/products/analysis_monitoring/ensostuff/ensoyears.shtml`

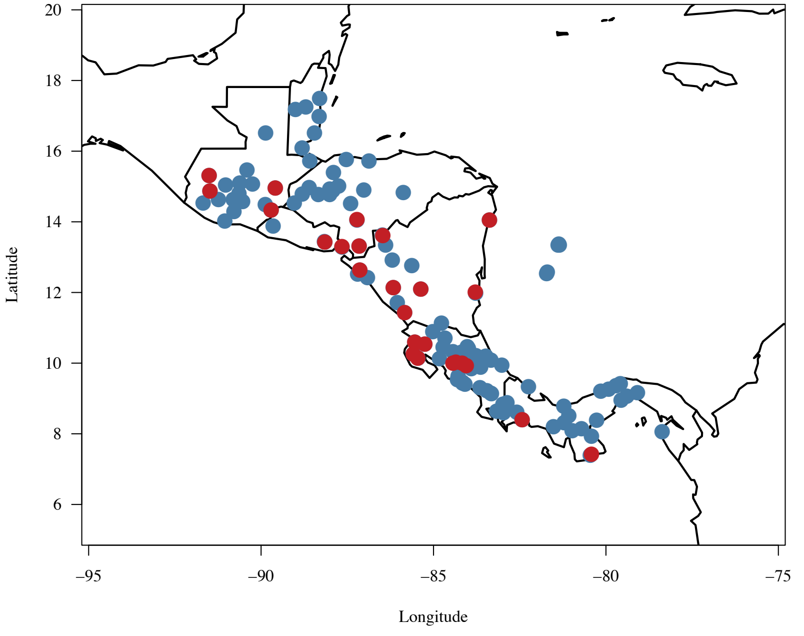

Figure 4.1. Spatial distribution of the gauge stations over Central America. The stations used in Paper II are in red. In Paper IV all the stations (blue and red) are used.

3-month running mean of SST anomalies in the Niño 3.4 region, based on centred 30-year base periods updated every 5 years.

5. Methods

5.1 Compositing ENSO and PDO

Composite analysis is performed in Paper I to study the influence of the PDO on the perturbation of the wind and precipitation. Table 5.1 also shows the classification into ENSO and the PDO phases according to CPC. The mean composite anomalies in this case are relative to the 61-year (i.e. 1950 – 2010) climatology for February. Notably, as for the general cases of ENSO, the cases are almost evenly distributed when one considers the combination of ENSO and PDO. This examination of ENSO and PDO events clearly differs from those conducted by, for example, Hoerling et al. (1997); Gershunov and Barnett (1998a); and DeWeaver and Nigam (2002). However, it does capture features that are important relative to the distribution of the ENSO and PDO events, such as the phase shift in La Niña events mentioned by DeWeaver and Nigam (2002). These authors also pointed out that the method used to calculate the composites does not influence the results of estimating the non-linear response of the ENSO events, being more important the distribution of the ENSO events.

5.2 Statistical Significance

In Paper I, the statistical significance for the composite analysis was tested using bootstrapping estimated in a way similar to that of Gershunov and Barnett (1998a). Using bootstrapping without replacement an artificial time series with normally distributed statistical noise is generated. The anomalies would then be considered significant at the 90% level if the absolute values exceed the 5th or 95th percentiles. A similar relationship between the absolute values of the anomalies was used to estimate the 95% and 99% confidence levels.

5.3 Detection of the MSD

In Paper II the daily precipitation times series were filtered using a running triangular weight average with a window of 31 days, to avoid or minimize interruptions of the MSD due to weakening of the trades and/or approaching of the ITCZ, as suggested by Ramírez (1983) and Alfaro (2014).

An algorithm to systematically identify the features of the MSD was applied to the filtered daily precipitation time series. This algorithm seeks for

Table 5.1. *Classification of ENSO events during February according to ONI. The PDO information is from http://jisao.washintong.edu/pdo (from Paper I).*

	High PDO	Low PDO
El Niño	1983, 1987, 1988, 1992	1953, 1954, 1958, 1959
	1995, 1998, 2003, 2010	1964, 1966, 1969, 1973
		1977, 1978
La Niña	1985, 1989, 1996, 1999	1950, 1951, 1955, 1956
	2000, 2001, 2006, 2008	1974, 1975, 1976
	2009	
Neutral	1981, 1982, 1984, 1986	1952, 1957, 1960, 1961
	1990, 1991, 1993, 1994	1962, 1963, 1965, 1967
	1997, 2002, 2004, 2005	1968, 1970, 1972, 1979
	2007	1980

the timing of each phase of the MSD (start, minimum, and end), besides the intensity and magnitude of the MSD. This approach provides an annual value for each quantity, which were used as indexes to characterize the MSD. The start of the MSD is considered as the moment when the decrease in precipitation initiates, usually after May-Jun. The end of the MSD is considered when the precipitation stops increasing, normally taking place around September-October. The minimum occurs in between the start and end of the MSD. The MSD intensity is defined as the minimum rainfall detected during the MSD (or the depth of the valley in Fig. 5.1), meanwhile the magnitude is the total precipitation divided by the total number of days between the start and end of the MSD.

5.4 Canonical Correlation Analysis

In Paper II, IV and V CCA (Wilks, 2011) is applied to investigate the variability of the MSD and precipitation anomalies during May-June and August-September-October, respectively. CCA is a statistical technique that searches for pairs of patterns in two multivariate data sets (fields), and constructs sets of transformed data variables by projecting the original data onto those patterns. These new variables maximize the interrelationships between the two fields. The new variables can be used, analogously to the regression coefficient in the multiple regression. The new variables or vector weights are also known as canonical vectors, and the projection with the respective fields as canonical variates. CCA can be useful in different applications, such as: i) to obtain diagnostic aspects of the coupled variability of two fields, in the case when the time series of observations of the two fields are simultaneous, or ii) to perform statistical forecasts, in the case when the time series of observations of

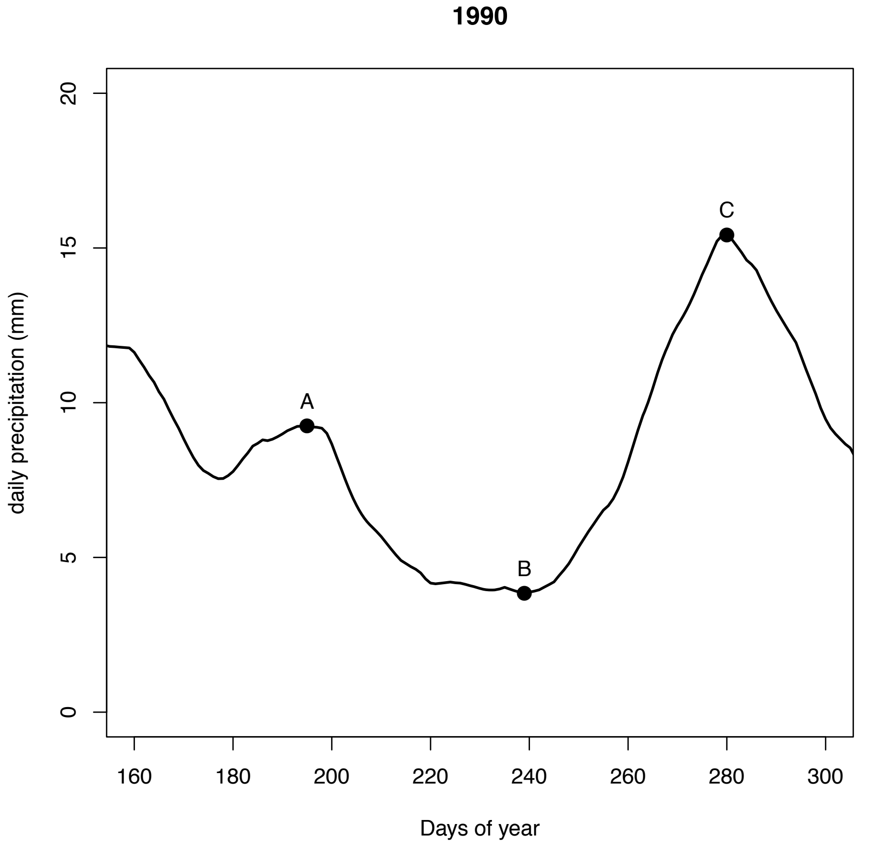

Figure 5.1. Filtered daily time series for the observed precipitation in station La Argentina during 1990. The dots represent the beginning (A), minimum (B) and end (C) of the MSD. In this year the MSD started by day 195 (14 July), reached the minimum at day 239 (27 August) and ended by day 280 (7 Oct). From Paper II.

one field precede the other (e.g. Alfaro 2007b; Maldonado and Alfaro 2011; Fallas-López and Alfaro 2012b, Paper V).

In Paper II, IV, and V CCA is used as a diagnostic tool, however, models for statistical forecasting can be built for future use. Consequently, CCA is employed in order to analyze the relationship between the SSTs monthly anomalies (SSTA, also denoted field X) and the indices characterizing the MSD and precipitation during May-June and August-October (each index would be the field Y, for the corresponding model), that is, it is sought a statistical relationship between the large and regional scale features of the SSTA and the characteristics of rainfall in all the stations (local scale).

In this approach, the fields (SSTA, MSD and precipitation indices) are first reduced by means of principal component analysis (PCA) to assure stability in the CCA parameters. A maximum of 17 EOFs and CCA modes in the filtering stage are allowed. This threshold was suggested by Gershunov and Cayan (2003) and Alfaro (2007b) to avoid over parameterization.

The optimal combination of EOFs and CCA modes are calculated by means of the goodness index (R^2, Fig. 6.5) . Notice that any set EOFs will produce unique CCA modes for that specific set, then, once the best combination of EOFs is determined, that set of EOFs, is capturing the maximum variability in each field (X and Y), separately, for each specific CCA model. The maximum possible number of CCA modes, however, is determined first by the minimum number of EOFs between both fields. Then with the goodness index, the maximum number of CCA modes is found for the best fit to avoid any parameterization in the model $\hat{Y} = b^T \cdot X$, where the elements of b are the ordinary least-squares regression coefficients computed with CCA, and $\hat{Y}$ is the predicted value of Y. The R^2 is computed using cross-validation models with 1-month window for the chosen period in each station for all the CCA models. This metric also allows identifying the best month to predict any of the MSD features. That is, the models would not necessarily have 17 EOF and CCA modes.

5.5 The Tropical North Atlantic Composites

In Paper IV, composites are estimated to diagnose to impact of the tropical North Atlantic (TNA) SST anomalies on precipitation changes during May-June. From the daily rainfall time series, four seasonal indices are estimated for every station, to describe the amount and time distribution of rainfall during May-June (MJ) through the period 1968-2012. The first index represent the total precipitation (TP) accumulated in MJ, the second show the frequency or occurrences of rainy days (FRD), and the last two, the average number of precipitation events exceeding the MJ 80$^{\text{th}}$ percentile (p80), and under the 20$^{\text{th}}$ percentile (p20), representing the wet and dry extremes, respectively.

Composites for SLP, wind at 850 and 200 hPa, relative humidity at 700 hPa, moisture flux 850 hPa, geopotential heights at 200 hPa, and total cloud coverage are estimated to analyze the atmospheric response to the SST forcing. The composites are calculated using the information obtained from the first CCA mode for the p80, which is associated with the TNA SST anomalies. The time series of this mode are categorized into three classes corresponding to the 33$^{\text{rd}}$ and 67$^{\text{th}}$ percentiles. The mode is considered below normal, and associated with colder than normal SST in TNA, if its annual value is less than that of the 33$^{\text{rd}}$ percentile. The opposite follows for values above the 67$^{\text{th}}$ percentile.

5.6 Experimental Design to Study SST Gradients Impact

In Paper III, a set of two experiments are carried out to study the impact of the meridional SST gradient at the Caribbean Sea on the intensification, formation and vertical structure of the CLLJ during winter and summer. The SST dataset used to force the atmospheric model is taken from the ERA interim project (Dee et al., 2011). In the control run (CR01, 5.2a) we force the atmospheric model with unmodified SST from 1990-01-01 to 2004-12-31. Then the SST dataset is modified to perform the next set of simulations. The experiment 1 (EX01, 5.2b) is run using the climatological SST calculated for the same period, thus, the model is forced with the twelve-monthly climatology for every year of the 15-year simulations. In experiment 2 (EX02, 5.2c), the original SST used in CR01 is modified over the area 10° – 17.5° N, 60° – 83° W (D01) in order to remove the influence of the meridional SST gradient. The gradient is almost suppressed with invert-distance weighted smoothing between the east and west boundaries of D01, where the meridional gradient is less intense.

The atmospheric model Integrated Forecast System (IFS, branch 36r4), provided by the EC-EARTH consortium (`http://www.ec-earth.org/`), and developed by the European Centre for Medium-Range Weather Forecast (ECMWF, `http://www.ecmwf.int/`) is used to carry out the experiments. The model is configured with a spectral resolution T255L91, which is approximately a 0.7×0.7 degrees of horizontal resolution and 91 vertical levels. The outputs are set to 16 levels below the 500 hPa.

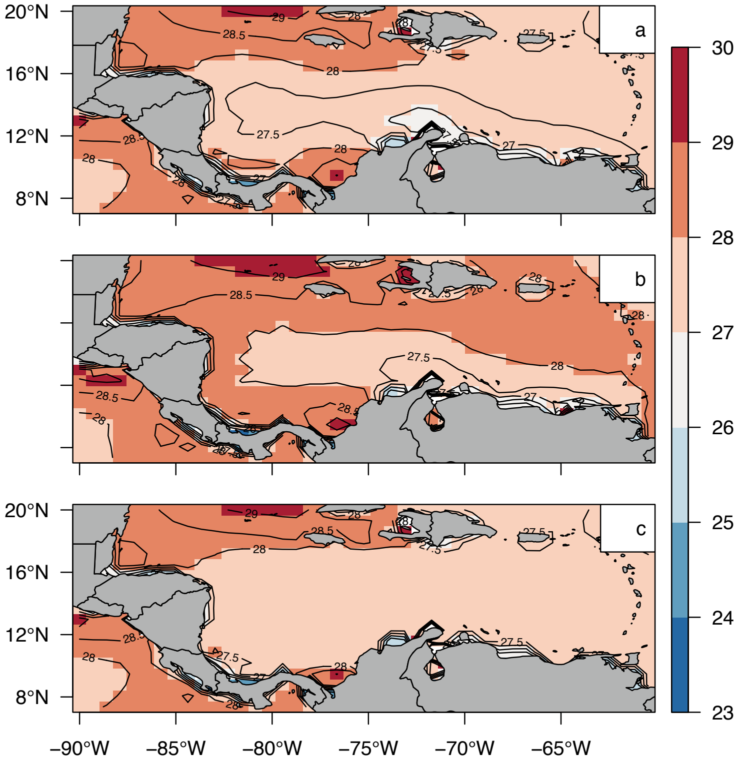

Figure 5.2. SST (°C) used as input for CR01 (**a**), EX01 (**b**) and EX02 (**c**). Panel (**a**) and (**c**) show the monthly mean SST for July 1994, while (**b**) shows the July SST climatology. The contour lines are spaced every 0.5 °C. From Paper III.

6. Results

In the next sections is presented a summary of the main results from the papers. Section 6.1 describes the interactions between El Niño and PDO reported in Paper I, while in Section 6.2 summarizes the outcomes from CCA models used in Paper II to study the MSD variability. In Section 6.3 the climate scenarios associated with anomalous SST in the TNA region are presented (Paper IV). Section 6.4 shows an extract from the experiments carried out in Paper III. Finally, Section 6.5 shows the validation of the heavy precipitation forecast for the season August-September-October 2010 made with CCA.

6.1 Influence of the PDO

Since the PDO is a long-lived phenomenon lasting approximately 30 – 40 years, a 30-year running average (not shown) was applied to the PDO index. This procedure reveals a negative PDO phase dominating from 1950 to 1981 and a positive PDO phase from 1981 to 2010. Table 5.1 lists the classification of El Niño and PDO phases. The anomalies are estimated relative to the climatology of the 61-year period from 1950 to 2010.

Figure 6.1a shows SLP anomalies (SLPA) for the El Niño and positive PDO (PDO+) sub-composite. Note a marked similarity with the spatial distribution of the SLPA pattern found for the El Niño composites (Paper II). Nevertheless, the SLPA are intensified and shifted south relative to El Niño case, while lower-than-normal pressure band is located over Central North America. These conditions enhance the Northern Hemisphere storms that reach low latitudes (Gershunov and Barnett, 1998b). This configuration of the SLPA spatial distribution is called a constructive pattern. In addition, significant negative SLPA (at 95 – 99% confidence levels) are located near each coast of North America, along with cyclonic circulation that weakens the trades and so, the CLLJ (Fig. 6.2a). Rainfall anomalies indicate drier-than-normal conditions over Central America and the Yucatan Peninsula and wetter-than-normal in southern Mexico (Fig. 6.3a). Significant anomalies in rainfall are found in south-western Mexico (positive), Nicaragua, and Panama (negative).

The other constructive case is that of La Niña and negative PDO (PDO-) Fig. 6.1d). Here, the spatial distribution of SLPA is similar to the SLPA pattern found in La Niña composites (Paper II). La Niña signal in the SLPA is modulated by the PDO-, producing more intense and extended SLPA. This condition can block storms from the north, preventing them from reaching

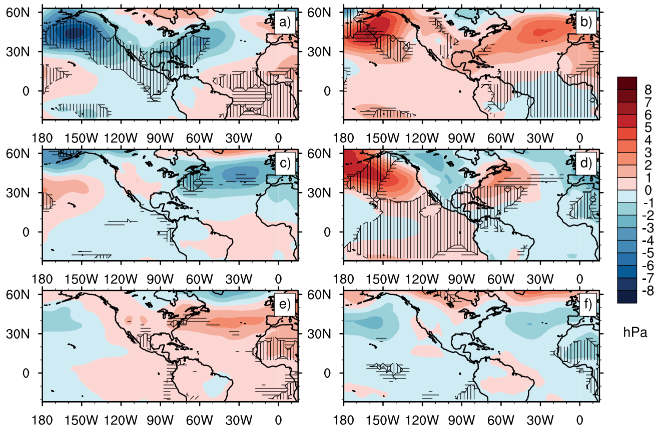

Figure 6.1. February mean SLP anomalies for the El Niño and PDO phase subcomposites: (**a**) El Niño and PDO+, (**b**) La Niña and PDO+, (**c**) El Niño and PDO-, (**d**) La Niña and PDO-, (**e**) neutral and PDO+, and (**f**) neutral and PDO-. Contours are spaced every 1 hPa. Shaded regions are significant anomalies with confidence levels of 90 – 95% (horizontal lines), 95 – 99% (vertical lines), and >99% (slant lines). From Paper I.

southern latitudes (Gershunov and Barnett, 1998b). Significant SLPA over the eastern North America are accompanied by anticyclonic circulation, enhancing the trades and the CLLJ (Fig. 6.2d). Rainfall anomalies present conditions that are drier-than-normal over Mexico and wetter-than-normal over Central America and the Yucatan Peninsula (Fig. 6.3d).

In the combination of El Niño with PDO-, or of La Niña with PDO+, the ENSO signal is modulated differently in comparison with the constructive cases mentioned above. Therefore, the condition in which ENSO and PDO are out of phase is regarded as a destructive pattern. Note that in Fig. 6.1b the spatial distribution of the SLPA is different from that of the constructive case (Fig. 6.1d), the high pressure anomaly centers being shifted to 160° W (over the north Pacific) and 30° W (north Atlantic). In the Atlantic, the trades are enhanced, and the wind over the Caribbean changes in direction (becoming south-easterly, Fig. 6.2b compared with the constructive case). Precipitation anomalies display similar distributions but with wetter conditions in Central America (Fig. 6.3b).

In the El Niño and PDO- case (Fig. 6.1c), the SLPA pattern is also distorted. In the Pacific, SLPA are located farther north. Their extent and intensity are decreased. In the Atlantic, SLPA (less intense) are located farther east. The circulation linked to the SLPA in the Atlantic does not greatly modify the trades over the Caribbean (Fig. 6.2c). Rainfall anomalies (Fig. 6.3c) display a distribution similar to that of their constructive counterparts, though south-

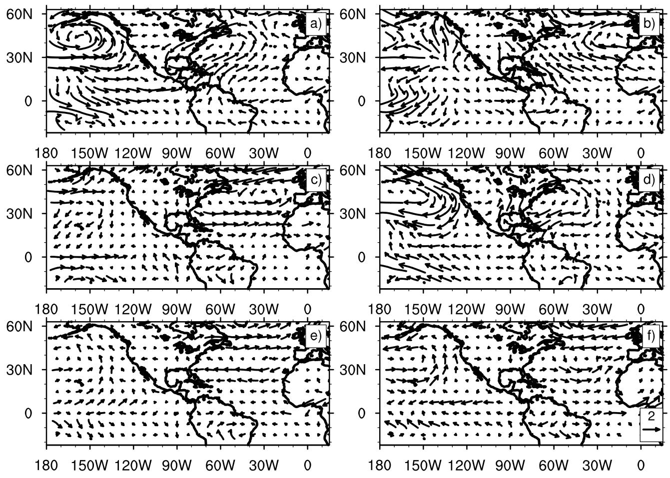

Figure 6.2. February horizontal wind anomalies at 925 hPa for (**a**) El Niño and PDO+, (**b**) La Niña and PDO+, (**c**) El Niño and PDO-, (**d**) La Niña and PDO-, (**e**) neutral and PDO+, and (**f**) neutral and PDO-. The reference vector is in ms $^{-1}$ (from Paper I).

western Mexico is drier than normal. Note that the rainfall anomalies are not statistically significant in Mexico or Central America.

The influence of the PDO on perturbations in the Central American climate is measured during neutral ENSO conditions (Fig. 6.1e and f). The SLPA spatial distribution in the Atlantic is similar during each phase, but with opposite sign. Consequently, the magnitude of SLPA is less than when combined with ENSO events. On the other hand, negative SLPA are found over the Pacific during each PDO phase, though negative SLPA are intensified during PDO- phase. Moreover, in each PDO phase, the observed SLPA do not produce marked changes in the horizontal wind at 925 hPa over the Caribbean (Fig. 6.2), so the association between the PDO and the perturbation in the CLLJ's intensity and direction is negligible or non-existent. Although the rainfall anomalies (Fig. 6.3e and f) tend to be positive during both PDO phases in most of the study domain, these results are not statistically significant.

The divergence field is shown in Fig. 6.4. In the constructive cases (Fig. 6.4a and d), the divergence anomaly pattern represents an intensification of the results found during both the El Niño and La Niña phases, besides having the opposite sign in each case. During El Niño (La Niña) positive (negative) anomalies are observed mainly over Costa Rica, Panama, and over the northeastern coast of South America, separated by negative (positive) anomalies over Colombia and Venezuela. In the destructive cases, however, each combination behaves differently. During the El Niño and PDO- case (Fig. 6.4c), larger changes are observed from 15° N towards the North Pole, over continental North America, and in the equatorial eastern Pacific. Note that the same region displays similar behavior in the changes on distribution of the precipi-

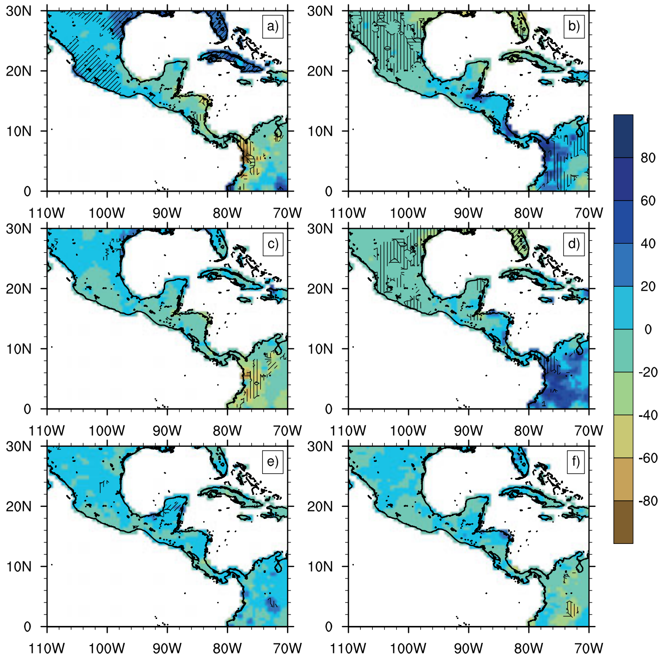

Figure 6.3. February anomalies of total monthly precipitation in millimetres (mm) for (**a**) El Niño and PDO+, (**b**) La Niña and PDO-, (**c**) El Niño and PDO-, (**d**) La Niña and PDO-, (**e**) neutral and PDO+, and (**f**) neutral and PDO-. Shaded regions are significant anomalies with confidence levels of 90 – 95% (horizontal lines), 95 – 99% (vertical lines), and >99% (slant lines), from Paper I.

tation anomalies (Fig. 6.3a and c). The other destructive case, i.e. La Niña and PDO+ (Figure 6.4b), occurs in a different manner: negative anomalies are intensified over Costa Rica, Panama, and South America, but significant positive anomalies are centred on 40° N and 90° W where reduced precipitation is observed. In the neutral cases, nevertheless, relevant changes happen only near the equator over continental South America. Regarding the influence of the PDO on rainfall, it is worth mentioning that the modulated divergence helps to explain some observed changes in the spatial distribution of precipitation, though there are other mechanisms related to combinations of the PDO with the Pacific North Atlantic (PNA) pattern and/or El Niño. These mechanisms are associated with changes in the distribution of the latent and sensible heat flux anomalies, modulating mainly the SST anomalies in the Gulf of Mexico (Muñoz et al., 2010) that could also be associated with changed precipitation distribution in the mid latitudes or with the changed storm tracks observed in the Northern Hemisphere by Gershunov and Barnett (1998a) and Zárate-Hernández (2013).

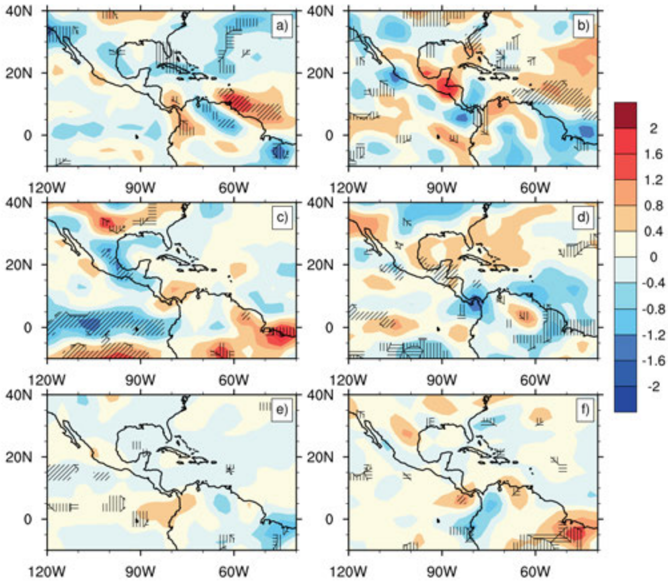

Figure 6.4. February divergence anomalies at 925 hPa for (**a**) El Niño and PDO+, (**b**) La Niña and PDO+, (**c**) El Niño and PDO-, (**d**) La Niña and PDO-, (**e**) neutral and PDO+, and (**f**) neutral and PDO-. Contours levels are spaced every 0.4×10^{-6} s^{-1} (from Paper I).

6.2 Influence of the SST on the MSD

Correlations of the MSD features with Niño 3.4 and the CLLJ indexes (Paper II) show that the MSD intensity and magnitude have a negative relationship with Niño 3.4 and a positive association with the CLLJ, however, for the Caribbean stations the results were not statistically significant, which is indicating that other processes might be modulating the precipitation during the MSD over the Caribbean side. On the other hand, the temporal variables (start, minimum and end) show low and no significant correlations with the same indexes.

Such results are also observed in models based on CCA. Using the SST anomalies as predictor (X field), CCA identifies SST patterns that are related to the perturbations of the MSD features (Y field, predictant). The goodness index (R^2) is shown in Fig. 6.5. The intensity and magnitude show the best skill score compared to the other indexes. These results show that the models to study the timing of the MSD phases have a poor performance using the CCA technique. Consequently, those models are not considered for further analysis. Both CCA models for MSD intensity and magnitude show one of the highest values of R^2 in April, which means in operational terms, information concerning the MSD intensity and magnitude can be retrieved up to 2 months in advance of an event. This would be valuable for preparation and planning of the societal, economical and agricultural activities during the MSD period. Notice that both intensity and magnitude models also shown the highest results in July, concurrently with the existence of the MSD, and CLLJ.

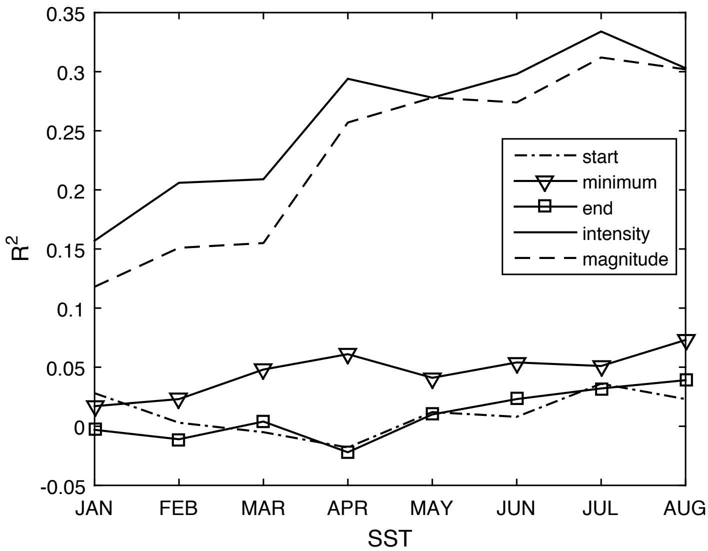

Figure 6.5. Goodness index (R^2) estimated as the average of the Pearson correlation between synthetic time series generated by cross-validation models and the observed MSD features per station (Paper II).

In Paper II, however, the SSTA patterns identified by the CCA in June are analyzed. The best combination of EOF and CCA modes for the MSD intensity are $X = 14$, $Y = 4$ EOFs and 2 CCA modes, and for the MSD magnitude $X = 11$, $Y = 6$ EOFs and 3 CCA modes, meaning that for each model (for intensity and magnitude respectively) the best fit is achieved when using 2 and 3 modes (canonical variates) respectively, capturing the maximum influence of the SST on the precipitation field, and specifically in the modulation of the MSD. For the scope of this thesis, only the results for mode 1 in both models are presented, however, higher order modes are explained in Paper II. Figure 6.6 shows the Pearson correlation between the predicted time series generated using cross-validation models and the observations of both intensity and magnitude in each station. In each case, the station exhibits relatively high significant correlation, about 0.35 in average.

The X loadings (correlation between the canonical vectors of the SST and the SSTA) of the first mode controlling the MSD intensity shows a bipolar pattern in the correlation with the SSTA surrounding Central America (Fig.

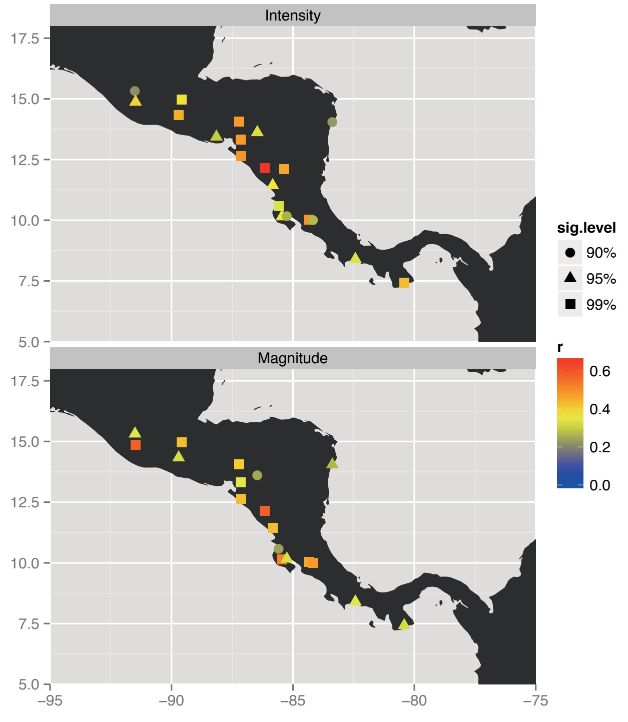

Figure 6.6. Pearson correlation of the CCA models with the time series of intensity (top) and magnitude (bottom) of MSD. Only significant correlations are plotted (Paper II).

6.7a,b). The highest positive correlations are found over the Pacific in the El Niño region, whereas the highest negative correlation are found over the Tropical North Atlantic and near to the Brazil coast. The influence of this variability mode on the precipitation in Central America has been previously studied by Enfield and Alfaro (1999); Maldonado and Alfaro (2010b, 2011) and Paper V, but for the secondary peak of precipitation during August-October (ASO), this result shows that the rainfall during the MSD is governed by the same variability mode present during the highest precipitation season in Central America. On the other hand, for the MSD magnitude, the first mode exerts more influence of the SSTA over the El Niño region, and the regional waters close to the west Mexican coast. Notice that in both cases also high positive correlations are found near the western coast of Mexico, revealing that both models are affected by the influence of regional waters, varying with the same phase that the superficial temperatures in the El Niño region.

The Y loadings in both models are negatively correlated with most of the stations (Fig. 6.7c,d). That means for a state in which the water over the Pacific is warmer (colder) than normal, plus the SST over the Atlantic colder (warmer) than normal, the intensity and magnitude of the MSD are increased (decreased) meaning drier (wetter) than normal conditions. This result also connects the MSD period with the second rainfall peak, that is, SSTs conditions for drier MSDs, would persist leading to less rainfall during the second peak, following the results in Paper V. The temporal scores (canonical variates) of this mode in both models show that this mode has mainly inter-annual variations (Fig. 6.7e,f).

6.3 Heavy precipitation events during May-June

The information obtained from CCA is used to examine the dynamical response of the atmosphere to anomalous SST over the TNA area. In this section the mode 1 from p80 CCA model (Fig. 6c, Paper IV) is used to estimate composites for SLP, geopotential heights at 200 hPa, horizontal moisture flux at 850 hPa, relative humidity at 700 hPa, and total cloud coverage. We choose this mode since it shows the highest correlation with the TNA (Table 1, Paper IV), besides it does not exhibit any relation with the Pacific indices. The classification of the TNA events is done accordingly to the time series of p80 mode 1 through the 33rd (p33) and 67th (p67) percentiles, so warm events of TNA are taken when this mode is above the p67. Then cold events are associated to values of the mode below the p33. The mean anomalies of the composites are estimated as the difference between the warm and the cold TNA events.

Figure 6.8a shows the 200 hPa heights response to warm anomalies over the TNA. The geopotential high associated with the tropical upper tropospheric trough (TUTT, Knaff 1997) is decreased due to positive anomalies centered between 20° – 30° N, 70° – 60° W. While the SLP (Fig. 6.8b) forms an anomalous low pressure just outside the Caribbean basin, near the Lesser Antilles. There is also an anomalous anticyclone located above 30° N and 70° – 80° W. The configuration at low levels could be associated to the Gills model (Gill, 1980) which predicts the formation of a low just to the northwest of the warming (Fig. 6.8c). This kind of configuration is known to decrease the vertical wind shear over the Caribbean Sea between the 850 hPa and 200 hPa (Knaff, 1997), improving the deep convection and the potential generation of tropical cyclones occurrences.

At mid-levels an increase of the relative humidity (Fig. 6.9a) is observed during warm TNA (Fig 6.8c). The decrease of the vertical wind shear, as above, enhances conditions for deep convection, causing an input increase of humidity from low levels. These results are also consistent with changes in the total cloud coverage (Fig. 6.9b). In northern Central America, nevertheless, the cloud coverage is higher than in the Caribbean, contrary to the results for humidity. This asymmetry suggest that the Caribbean is not the only moisture source due to the TNA events, as pointed out by Durán-Quesada et al. (2010).

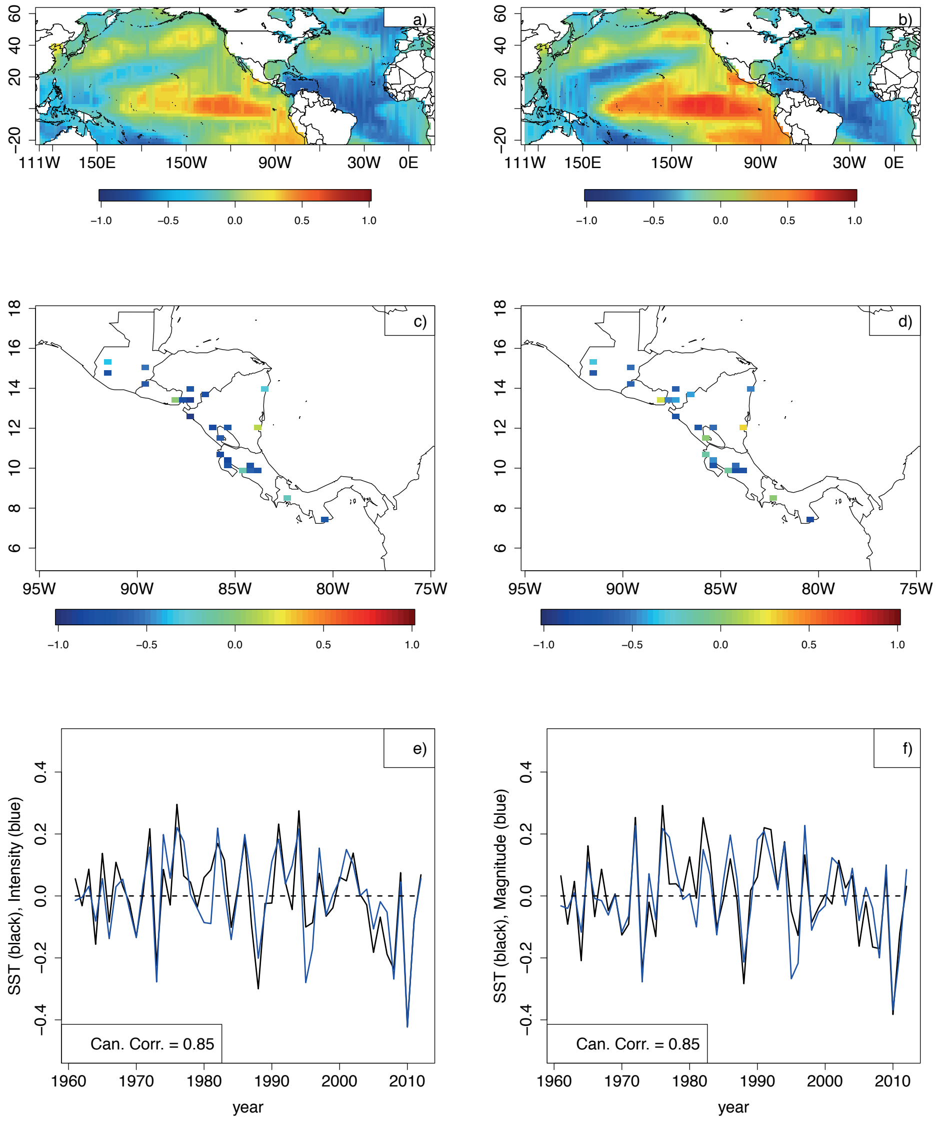

Figure 6.7. CCA mode 1 for both MSD intensity and magnitude. In the left column are the X (upper) and Y(middle) loadings, and the time scores (bottom) for the intensity. In the right column the same but for the magnitude (Paper II).

Notice that these conditions in the Caribbean Sea favors also the formation of tropical cyclones in the basin (Alfaro, 2007a).

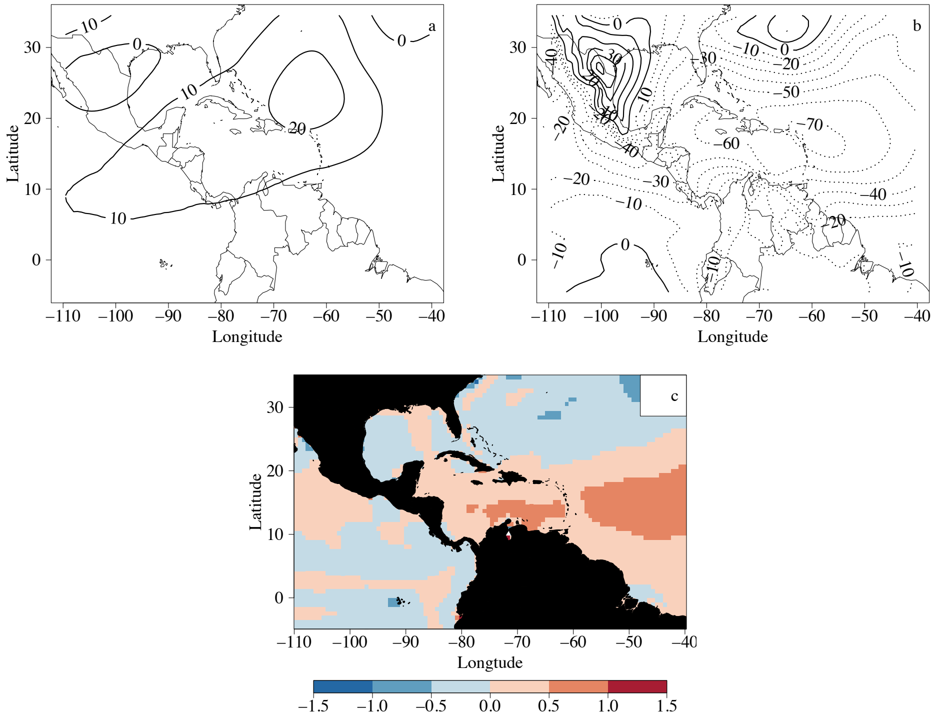

Figure 6.8. May-June composites of warm minus cold tropical North Atlantic (TNA) events using the ERA-Interim products of geopotential heights at 200 hPa (**a**) and SLP (**b**) and SST (**c**). The contours are spaced each 10 Pa or m. Solid lines represent positive anomalies, dashed lines show negative anomalies. (Paper IV).

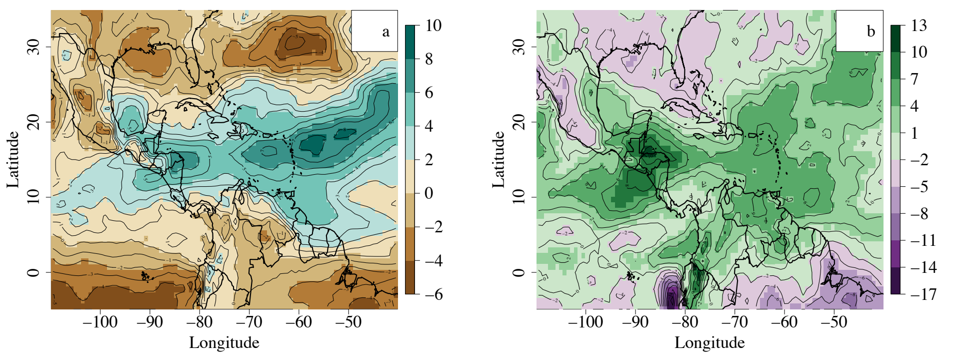

Figure 6.9. Same as Fig. 6.8, but for the relative humidity at 700 hPa (**a**) and total cloud coverage (**b**). Both units are in percentage (Paper IV).

To examine the anomalous moisture sources for Central America, Fig. 6.10 shows the horizontal moisture flux divergence, calculate as

$$\nabla(q \cdot \mathbf{V}) = \mathbf{V} \cdot \nabla q + q(\nabla \cdot \mathbf{V}),$$

where q is the specific humidity and $\mathbf{V}$ the horizontal wind vector. Due to the anomalous westerly circulation formed at low levels (Fig. 6.8b), it provokes an increase of moisture flux from the Pacific to northern Central America (El Salvador, Guatemala). In the Caribbean side, there is an increase in the moisture convergence located over Nicaragua, Guatemala and Honduras. This anomalous flux from the Pacific plus the mean moisture input from the Caribbean (Durán-Quesada et al., 2010), may enhance the conditions to form meso-scale systems affecting Central America, explaining also the increase in cloudiness over the region.

These findings help to explain the observed simultaneity of the rainy season in Central America in northern and southern locations (see for example Magaña et al. 1999; Amador et al. 2006, 2016). The mean position during MJ of the ITCZ contributes to the formation of precipitation events in the southern part of Central America. On the other hand, a relative warming (cooling) of about 0.5 °C of the SST over the TNA provokes the decrease (increase) of the vertical wind shear plus formation of anomalous westerly (easterly) circulation. During warm TNA events, an increase of humidity at mid-levels is observed in the Caribbean, in addition to an augmentation of the humidity transported from the Pacific to Central America improving the conditions for the formation of rainy systems during May-June.

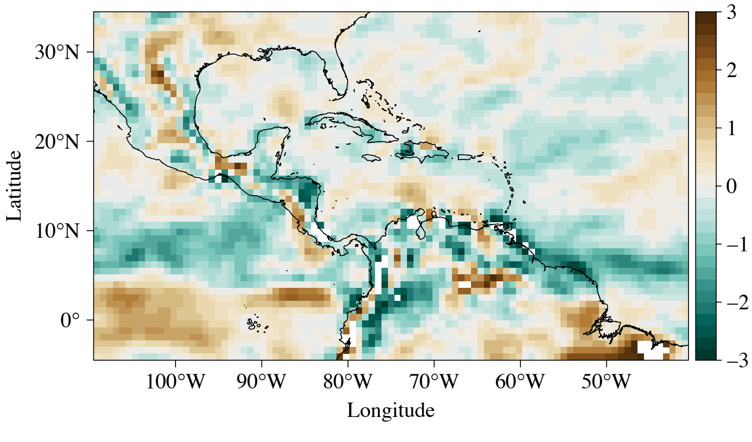

Figure 6.10. Same as Fig. 6.8, but for the horizontal moisture divergence at 850 hPa. Color levels are multiplied by 1×10^8. Units are in kg kg^{-1} m s^{-2} (Paper IV).

6.4 Impact of the Meridional SST gradient on the CLLJ

6.4.1 Sea level pressure and CLLJ

In order to examine the baroclinic structure of the CLLJ, we calculated the SLP and the zonal wind at 925 hPa areal averages over the region bounded by 12.5° – 17.5° N and 80° – 70° W, where the jet core is located. The SLP observed in ERA-interim reproduce a semi-annual cycle previously reported by Wang (2007), with SLP peaking in winter and summer (Fig. 6.11a). This seasonality is attributed to the seasonal migration of the NASH. The SLP semi-annual cycle is also visible in all the three simulations.

The meridional SLP gradient (Fig. 6.11b) and the zonal wind (Fig. 6.11c) also show the same seasonality noted for the mean SLP in all the simulations. Furthermore, the peaks of the meridional SLP gradient coincide with the peaks of the CLLJ. According to Wang (2007), the meridional SST gradient in this region is coupled with the atmospheric boundary layer in such a way that it can induce the observed meridional SLP gradient associated to the CLLJ. While all these variables show a close relationship for all simulations, the results from the sensitivity experiment (EX02) in which we removed the meridional SST gradient over the Caribbean Sea, suggest that the meridional SST gradient is not the main cause for the observed gradient in SLP, and therefore it is not involved in the consequent acceleration of the wind at low-level that generates the CLLJ.

In contrast, the average meridional SST gradient over the Caribbean is generated due to the interaction of the CLLJ with the sea waters through dragging and friction forces (Amador, 2008). Once the gradient is established, this interaction enhances the CLLJ and vice versa through the conceptual model proposed by Lindzen and Nigam (1987). The results of the experiment EX02 strongly suggest that the meridional SST gradient alone is not sufficient to explain the jet formation. This is consistent with Ranjha et al. (2013), who also found that the CLLJ origin cannot be associated to the thermal contrast between land and sea neither in winter nor summer. Hence, our results do not support the hypothesis brought forward by Muñoz et al. (2008) and Cook and Vizy (2010) on the influence of the mountains on the CLLJ's core strength through the land-sea thermal contrast.

6.4.2 Impact on Precipitation

All the simulations underestimate precipitation over the Caribbean Sea (7° – 20° N; 95° – 75° W) compared to reanalysis (Fig. 6.12a). In addition, precipitation in every experiment is similar to CR01. The MSD is well developed in every simulation between July and August in agreement with reanalysis. These findings further corroborate the fact that both the meridional SST gradient over the Caribbean Sea and the mountains over the NSA edge have minor impact on the climate of the region in contrast to what was pre-

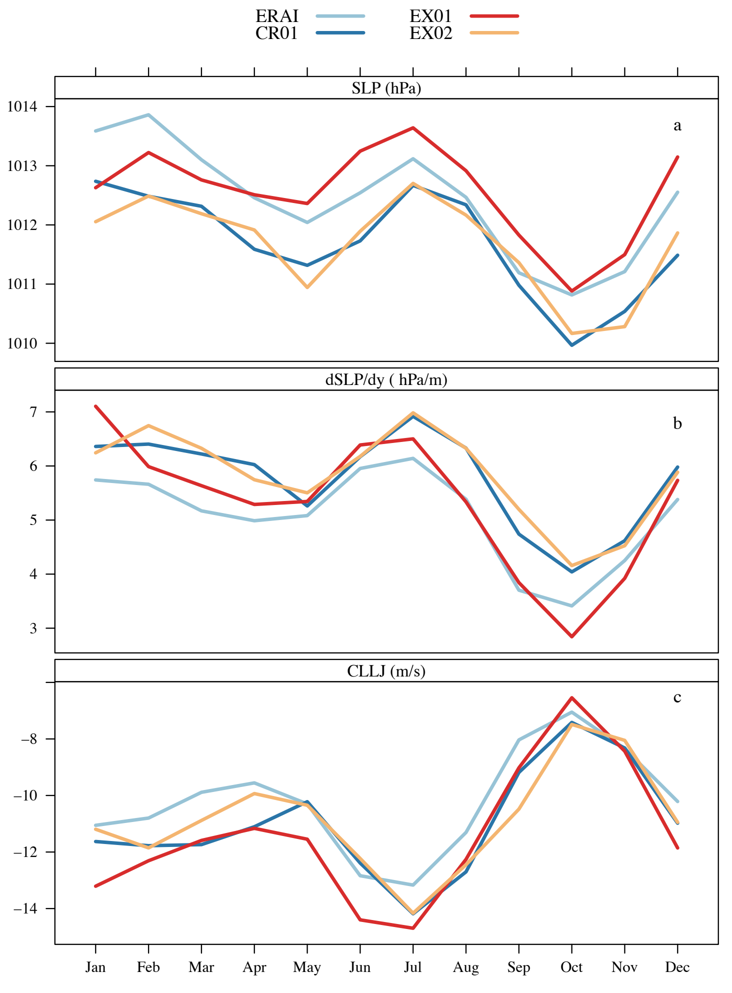

Figure 6.11. Annual cycle of the (**a**) mean SLP, (**b**) meridional SLP gradient and (**c**) zonal wind at 925 hPa, in the area bounded by 12.5° – 17.5° N and 70° – 80° W (Paper III).

viously thought (Wang, 2007; Cook and Vizy, 2010; Chang and Oey, 2013). The latter is explained by the fact that in none of the experiments the CLLJ has changed significantly to impact the vertical wind shear and the moisture transport, which are known to be related with rainfall production in the region, resulting in modifications to the hydrological cycle. Saying that, some discrepancies among the simulations might arise due to the fact that the average includes regions located in the Pacific and Caribbean basins, and not necessarily the annual cycle of precipitation in these areas is the same. Other differences may be also related to the sensitivity of the model to ENSO, i.e, in the simulation EX01, the ENSO influence is suppressed, therefore, the results might vary in comparison to the CR01, and EX02, where the ENSO signal is kept.

To further investigate the precipitation discrepancies found in the EX01 experiment, we estimated the composites of El Niño, La Niña and neutral years for precipitation, using the information in Section 2. During neutral years (Fig. 6.12b), the CR01 shows that the annual cycle of rainfall is modeled properly, depicting a first peak during May-June and a second maximum by October. EX01 shows drier conditions in July during neutral years. The El Niño composites (Fig. 6.12c) show that by removing the El Niño signal from the input data (EX01), the response of the model is to estimate about the same precipitation rate in average, however, wetter condition are found from July to September. On the other hand, the impact on rainfall of La Niña signal (Fig. 6.12d) does not necessarily oppose the El Niño effects. EX01 shows drier conditions from June to November compared to CR01, while in EX02 the reduction is observed from May to August. One particular feature common among the La Niña composites in the simulations is the absence of the MSD, due to wetter conditions during La Niña. These results reveal a non-linear response of precipitation to ENSO events (Hoerling et al. 1997, Paper I) which is captured in the model.

6.5 Validation of CCA Forecasts

In Paper V, CCA has been used to estimate seasonal forecasts of precipitation in ASO, using SSTA as predictor. The results show that the main variability mode controlling precipitation during ASO, is a dipole formed between the SST over the equatorial Pacific Ocean and TNA region. This pattern was also observed to control the intensity and magnitude of the MSD (Paper II).

CCA forecasts for precipitation in ASO are validated against meteorological observations and natural disaster reports for the ASO 2010. During July 2010, La Niña conditions were developed across the central and eastern equatorial Pacific Ocean. Figure 6.13 shows that, in addition, to colder temperatures in the Pacific Ocean, relative warmer than normal SSTA are found in the Caribbean Sea. According to the CCA models, this SST pattern is associated to a wetter than normal season. A validation of the forecast for total precipitation in ASO, using stations mainly located in Costa Rica, shows that the forecasts have good accuracy compared to the observations, according to the predicted and observed categories (Table 6.1). This climate scenario and the forecast, including the probable impacts, was explained by the author at the Central American Regional Climate Outlook Forum (CARCOF, García-Solera and Ramirez 2012) celebrated in San Salvador, El Salvador in July 2010, and was one of the inputs used to produce the consensus outlook map for ASO 2010.

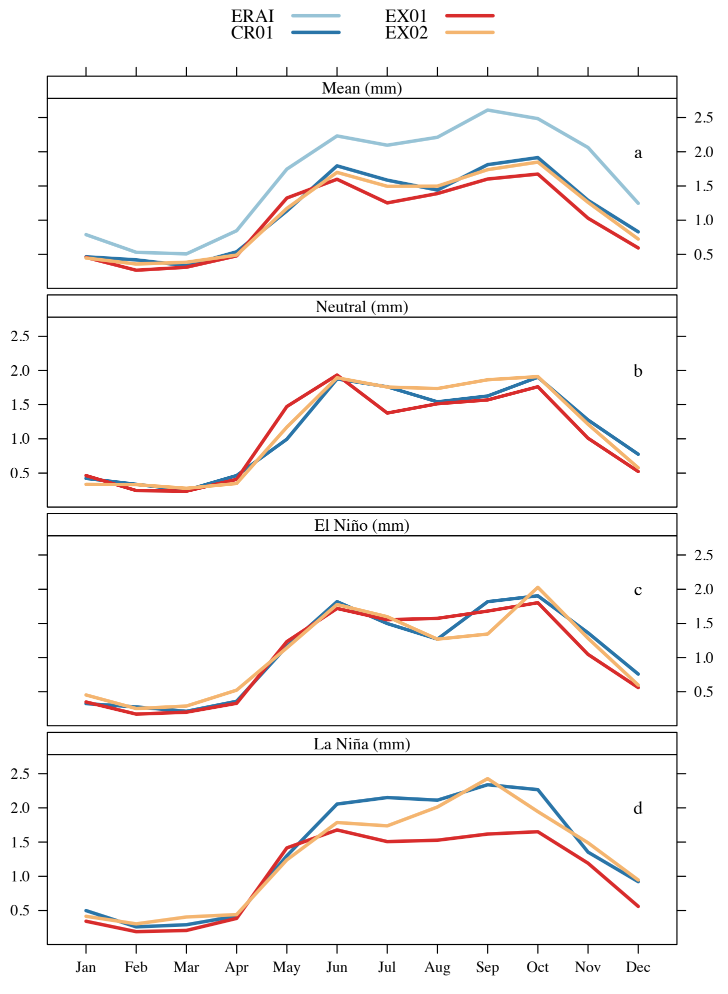

Figure 6.12. Annual total precipitation cycle (mm day^{-1}) in the area bounded by 7° – 20° N and 75° – 95° W. (**a**) Shows a comparison amongst the experiments and reanalysis. Composites of the neutral (**b**) El Niño (**c**), La Niña (**d**) years (Paper III).

However, the information from natural disaster reports does not necessarily match the above mentioned results (Fig. 6.14). For example in regions such as Guanacaste, northwest Costa Rica, most of the stations (e.g. Nicoya, Santa Cruz, Bagaces) registered a total precipitation scenario above normal in both observation and forecast, nevertheless, few total impacts reports are found. Contrary to this, San José (where about 50% of the country's population lives) shows a higher rate of natural disaster reports, with rainfall scenarios between normal and above normal. This fact reflects the importance of including other variables to study and forecast the impact of natural disasters in the region,

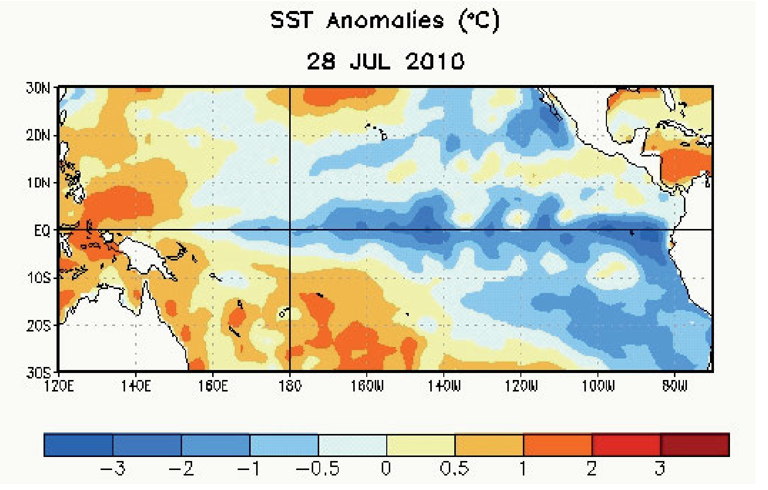

Figure 6.13. Average SSTA (°C) for the week centered on 28 July 2010. Anomalies are computed with respect to the 1971-2000 base period weekly means (Xue et al., 2003). Taken from `http://www.cpc.ncep.noaa.gov/products/analysis_monitoring/enso_disc_aug2010/figure1.gif` (Paper V).

Table 6.1. *Validation of total precipitation accumulates (TP) forecast for ASO 2010. The observed values were reported by 5 gauge stations from Costa Rican Meteorological and Hydrological Services. Categories are below- (B), normal (N) and above- (A) than-normal (Paper V).*

Station	Lon	Lat	Obs. (mm)	Obs. cat.	Forecasted cat.
Nicoya	-85.45	10.15	1202.00	A	A
Santa Cruz	-85.33	10.02	944.00	A	A
Bagaces	-85.25	10.53	790.00	A	A
CIGEFI	-84.05	9.94	1018.00	N	A
Aerop. J.S.M.	-84.22	10.00	1072.00	A	A

since using only climatic elements gives an approximate, but not complete overview of the issue.

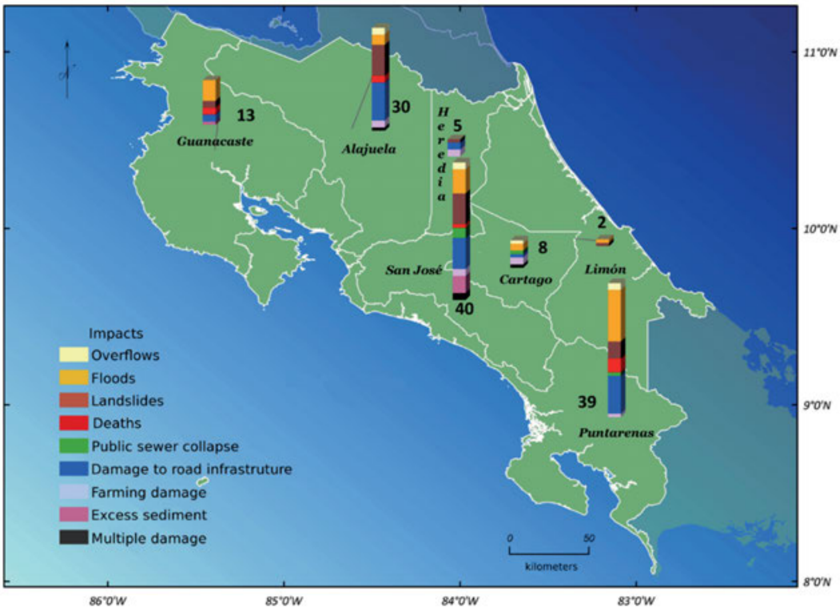

Figure 6.14. Spatial distribution, by province, of the impacts and disasters due or related to hydro-meteorological causes during ASO 2010 season. Numbers are the sum of the categories listed and were collected from Costa Rican main newspapers. From Paper V.

7. Conclusions

In this thesis, several statistical techniques have been used for the analysis of the main variability elements associated to rainfall fluctuations in Central America. A set of sensitivity experiments using a global atmospheric model, has been done in order to analyze the impact of SST anomalies on climate elements such as the CLLJ and precipitation. Four main conclusions are drawn from the results presented in this study and are listed below:

- In winter it is found that ENSO events are connected to CLLJ anomalies by modulating the SLP near the east coast of the United States and the Aleutian Low. During warm (cold) ENSO phases, negative (positive) anomalies in the SLP field over the east coast of North America produce cyclonic (anticyclonic) circulations at low levels. The results indicate that when the ENSO and PDO are in phase (out of phase), the SLP anomalies signal is enhanced (weakened or cancelled), affecting the CLLJ anomalies in both direction and intensity, and also changing the spatial distribution of precipitation.

- It is found that the meridional SST gradient has a minor impact in the jet structure, contrary to previous reports, therefore the mechanisms involved in the CLLJ structure, intensification and decrease remain as a scientific challenge.

- The MSD intensity and magnitude show a negative relationship with Niño 3.4 and a positive relationship with the CLLJ index. However in the Caribbean stations the results were not statistically significant, which indicates that other processes could be modulating the precipitation during the MSD over the Caribbean side.

- The results from CCA show good performance to study precipitation anomalies from May to October. This technique shows potential ability for forecasting heavy precipitation events during May-June and August-October, and also to predict the MSD intensity and magnitude, using SST anomalies as predictor. The validation against meteorological observations and natural disaster reports related to hydro-meteorological events, shows that the methodology has good agreement with the observed precipitation, yet the forecast and observations do not necessarily match the natural disaster reports.

8. Summary

The present thesis consists in a main chapter and five scientific papers, denoted in roman number. The interaction between El Niño and the PDO was studied in Paper I using composite analysis. The interaction between these two variability modes during boreal winter is summed up as follows:

- During warm (cold) events, the SLPA align with the PNA teleconnection pattern, and cyclonic (anticyclonic) circulation is observed, resulting in westerly (easterly) wind anomalies over the Caribbean Sea, weakening (enhancing) the jet intensity. The PDO enhances or attenuates the ENSO signal in the SLPA (i.e. during El Niño events concomitant with a positive PDO, the PNA teleconnection pattern is enhanced), whereas during El Niño in combination with negative PDO, the PNA pattern is not observed, resulting in no significant modification of the circulation over the Caribbean Sea.

- Changes in the circulation due to the PDO phases during La Niña episodes are observed in the direction change of the meridional wind anomalies in the Caribbean basin. Cold events plus positive (negative) PDO result in an anomalous northward (southward) wind component.

- Despite large changes in the circulation pattern found due to the influence of the PDO, changes in the monthly cumulative precipitation anomaly were minimal over the Central American Isthmus. The small perturbations in rainfall were related to small fluctuations in the divergence in the tropical regions of the American continent.

In Paper II it is found that the SST anomalies control the MSD intensity and magnitude. The results show that:

- the MSD intensity is mainly modulated by a bipolar configuration in the SST anomalies formed between the Pacific and the Tropical North Atlantic and Caribbean sea, meanwhile, the first mode controlling the MSD magnitude shows more influence from El Niño and the regional waters close to the western coast of Mexico and Central America. This variability mode in both models has an inter-annual scale, with negative effects in precipitation, i.e. when this mode is positive for both intensity and magnitude, a reduction in rainfall is observed in almost all the stations. Similar SST dipole has been reported to influence the anomalies in rainfall during the months of the highest precipitation events (August-November), and it has been associated with intensification/reduction of the trades, leading to a decrease/increase of precipitation in Central America during the second rainfall period, however, these results show that this mode is present prior to the quarter ASO and is also modulating the precipitation during boreal summer.

- The CCA allows identifying patterns of the SST affecting variables describing the MSD, such as the intensity and magnitude, however, it shows a poor performance related to the temporal variables. Another benefit achieved using CCA was the identification of particular months suitable for prediction of the intensity and magnitude of the MSD, being capable of forecasting up to two months in advance, which is a reasonable time in terms of practical matters related to prevention and planning for the season. Finally, it is worth pointing out that this analysis also provides a systematic method to study the MSD features, that can be used for statistical forecasts of such a phenomenon.

Paper III shows that the impact of the meridional SST gradient on the CLLJ is minimal. Two main conclusions are drawn from those findings:

- Despite the evidence of its baroclinic structure, from the sensitivity experiments results, this hypothesis does not succeed explaining the jet intensification during winter and summer. On the other hand, barotropically unstable conditions in the Caribbean, are observed throughout the year, not only in summer as shown by Molinari et al. (1997) and Amador (1998, 2008); therefore, it can be presumed that wave-like processes such as the cold outbreaks and surges in the Caribbean in winter or the easterly waves in summer, can instead be interacting with the CLLJ.

- Precipitation in Central America is mainly modulated by large-scale elements such as ENSO phases through its teleconnections (Amador et al. 2006; Amador 2008, Paper I), rather by latitudinal differences of the SST in the Caribbean Sea.

The results from Paper IV show that the heavy rainfall events during May-June are associated with SSTA over the TNA region in such a way that:

- The TNA SST warm (cold) anomalies modulate the pressure field (associated with the TUTT), producing changes in low-level circulation decreasing (increasing) the easterlies for warming (cooling) of SSTs west to the African coast. This modulation is associated to wetter (dryer) conditions in Central America.

- Under warm SST anomalies over the TNA, an increase of relative humidity over the Caribbean is found, in addition to a decrease in the vertical wind shear, enhancing deep convection activity and favoring conditions for cyclone-genesis.

- Anomalous moisture flux from the Pacific that reaches the Central American coast, may improve the conditions for formation of mesoscale convective systems, due to the interaction of the flux with topography.

Paper V provides a validation of seasonal precipitation forecasts using CCA and the results reveal that:

- Prediction of heavy precipitation events are linked to the state of the SST in the eastern and central equatorial Pacific Ocean, and the TNA region, being the dipole formed by the contrast of SST in these areas, the main variability mode explaining extreme rainfall during ASO.

- Derived models from CCA have high accuracy for seasonal forecasting of precipitation in Central America. However, in terms of natural disasters with hydro-meteorological origin, the technique does not provide a complete overview of the events. Other variables are needed for a comprehensive understanding of these catastrophes.

9. Outlook

Seasonal forecast of precipitation in Central America is extremely relevant for the region, due to the impact of rainfall fluctuations on environment and society. Currently regional climate outlook fora are carried out in the area, thrice a year for each of the rainfall periods discussed in this thesis, i.e. January-February, May-June and August-September-October. In those fora several stake-holders meet in order to make a regional plan for every season (Donoso and Ramírez, 2001; García-Solera and Ramirez, 2012). This thesis contributes providing a systematic method, which has proven to be useful not only for seasonal precipitation forecast but also for analysis of large and regional scale conditions previous to the months of interest.

A better understanding of a long-lived phenomenon like PDO improves our knowledge on climate variability, but also the notion of climate change. A PDO phase change can occur only once for a normal human life. The impact of such a phase change could alter the current climate conditions, modifying the perception of what we know as "*normal climate conditions*". The PDO has shown statistical evidence of interaction with ENSO events during winter, when both elements peak. However, PDO has been also found to be involved in the heavy precipitation events during spring and summer, however, the mechanism connecting the PDO with changes in precipitation upon Central America during spring and summer remain unknown. This thesis provides an experimental setup, using global atmospheric models, that can be employed to thoroughly analyze the dynamics and PDO impact on the climate over the region, and the evolution of this process in the future.

While CCA has shown an adequate performance for forecasting precipitation using SST as predictor, other variables such as humidity (specific or relative) might be included as predictor in future analyses to improve rainfall forecasts. Nonetheless, in this thesis it is shown that extreme precipitation event studies need an integrated framework involving several disciplines to assess the impact of those rainfall episodes on society.

The use of a high resolution global atmospheric model has already proven to be an important tool for understanding the climate, specially in areas such as Central America, where regional features become important for climate and weather. The numerical experiments achieved during this work have shown the potential of these models for both the studies of complex climate processes such as the CLLJ, and for the dynamic perspective in which statistical models, obtained using CCA, are complemented.

10. Acknowledgements

The work in which this thesis is based, would not be possible without the help and support that many people have shown me during my four years as a PhD student. I would like to give special thanks to my supervisors Anna Rutgersson, Eric Alfaro, Jorge Amador and Björn Claremar. Thanks for your patience, guidance, for always encourage me to achieve this goal, and for keeping me down-to-earth during all this time.

I would like to thank all the co-authors of the papers, Rodrigo Caballero, Franceso Salvatore Rocco Pausata, Luis Alvarado and Berny Fallas.

I would like to thank all the present and former meteorology PhD fellows: Olof, Johan, Erik, Eva, Andreas, Adam, Lichuan, Nina, Jenny, Kristina and Antoine for sharing your laughs and experiences. Special thanks to Leif, Taher, Anna, Erik, Fredrick and Tomas.

This doctoral thesis was carried out within the framework of the Centre Natural Disaster Science research school, supported by the Swedish International Development Cooperation Agency (Sida) through their contract with the International Science Programme (ISP) at Uppsala University (contract number: 54100006). The author would like to give special thanks to Klaus Wyser and Hamish Struthers and the Swedish National Infrastructure for Computing (SNIC) for their help and technical support. The author would also like to thank the project 805-A9-532 / 805-B0-065 / 805-B0-130 / 805-B3-600 / 805-B4-226 / 805-B4-227 / 805-B6-143 / 805-B5-296 CIGEFI-UCR and to the Central American National Weather and Hydrology Services that provided the rainfall data used in this work.

References

Alfaro, E., L. Cid, and D. Enfield, 1998: Relaciones entre la precipitación en Centroamérica y los Océanos Pacífico y Atlántico Tropical. *Investigaciones Marinas*, **26**, 59–69.

Alfaro, E. J., 2000: Eventos cálidos y fríos en el Atlántico tropical norte. *Atmósfera*, **13 (2)**, 109–119.

Alfaro, E. J., 2007a: Escenarios climáticos para temporadas con alto y bajo número de huracanes en el atlántico. *Revista de Climatología*, **7**, 1 – 13.

Alfaro, E. J., 2007b: Uso del análisis de correlación canónica para la predicción de la precipitación pluvial en Centroamérica. *Ingeniería y Competitividad*, **9 (2)**, 33–48.

Alfaro, E. J., 2014: Caracterización del "veranillo" en dos cuencas de la vertiente del Pacífico de Costa Rica, América Central (Characterization of the Mid Summer Drought in two Pacific slope river basins of Costa Rica, Central America). Spanish. *International Journal of Tropical Biology*, **62 (4)**, 1–15.

Alfaro, E. J. and L. Cid, 1999a: Ajuste de un modelo VARMA para los campos de anomalías de precipitación en Centroamérica y los índices de los océanos Pacífico y Atlántico Tropical. *Atmósfera*, **12**, 205–222.

Alfaro, E. J. and L. Cid, 1999b: Análisis de las anomalías en el inicio y el término de la estación lluviosa en Centroamérica y su relación con los océanos Pacífico y Atlántico Tropical. *Tópicos Meteorológicos Oceanográficos*, **6**, 1–13.

Alfaro, E. J. and J. Cortéz, 2012: Atmospheric forcing of cool subsurface water events in Bahía Culebra, Gulf of Papagayo, Costa Rica. *Revista de Biología Tropical*, **60**, 173 – 186.

Alfaro, E. J. and P. M. Pérez-Briceño, 2014: Análisis del impacto de fenómenos meteorológicos en Costa Rica, América Central, originados en los mares circundantes. *Revista de Climatología*, **14**, 1 – 11.

Alfaro, E. J., A. Quesada, and F. Solano, 2010: Análisis del impacto en Costa Rica de los ciclones tropicales ocurridos en el mar Caribe desde 1968 al 2007. *Diálogos Revista Electrónica de Historia*, **11 (2)**, 22–38.

Alfaro, E. J. and J. Soley, 2009: Descripción de dos métodos de rellenado de datos ausentes en series de tiempo meteorológicas. *Revista de Matemáticas: Teoría y Aplicaciones.*, **16 (1)**, 59–74.

Amador, J. A., 1998: A Climatic Feature of the Tropical Americas: The Trade Wind Easterly Jet. *Tópicos Meteorológicos y Oceanográficos.*, **5 (2)**, 91–102.

Amador, J. A., 2008: The Intra-Americas Sea Low-level Jet Overview and Future Research. *Annals of the New York Academy of Sciences*, **1146 (1)**, 153–188, doi:10.1196/annals.1446.012.

Amador, J. A. and E. Alfaro, 2009: Métodos de reducción de escala: aplicaciones al tiempo, clima, variabilidad climática y cambio climático. *Revista Iberoamericana de Economía Ecológica (REVIBEC)*, **11**, 39–52.

Amador, J. A., E. J. Alfaro, O. G. Lizano, and V. O. Magaña, 2006: Atmospheric forcing of the eastern tropical Pacific: A review. *Progress In Oceanography*, **69 (2–4)**, 101–142, doi:10.1016/j.pocean.2006.03.007.

Amador, J. A., E. J. Alfaro, E. R. Rivera, and B. Calderón, 2010: Climatic Features and Their Relationship with Tropical Cyclones Over the Intra-Americas Seas. *Hurricanes and Climate Change*, Springer Netherlands, Netherlands, Vol. 2, 149–173.

Amador, J. A., J. R. Chacón, and S. Laporte, 2003: Climate and climate variability in the Arenal Basin of Costa Rica. *Climate, Water and Trans-boundary Challenges in the Americas*, H. Díaz and B. Morehouse, Eds., Kluwer Academic Publishers, Holland, 317–349.

Amador, J. A., A. M. Durán-Quesada, E. R. Rivera, G. Mora, F. Sáenz, B. Calderón, and N. Mora, 2016: The easternmost tropical Pacific. Part II: Seasonal and intraseasonal modes of atmospheric variability. *Revista de Biología Tropical*, **64 (1)**, S23 – S57.

Bell, G. D. and M. Chelliah, 2006: Leading Tropical Modes Associated with Interannual and Multidecadal Fluctuations in North Atlantic Hurricane Activity. *Journal of Climate*, **19 (4)**, 590–612, doi:10.1175/JCLI3659.1.

Chang, Y.-L. and L.-Y. Oey, 2013: Coupled Response of the Trade Wind, SST Gradient, and SST in the Caribbean Sea, and the Potential Impact on Loop Current's Interannual Variability. *Journal of Physical Oceanography*, **43 (7)**, 1325–1344, doi:10.1175/JPO-D-12-0183.1, wOS:000329778000006.

Chen, A. A. and M. A. Taylor, 2002: Investigating the link between early season Caribbean rainfall and the El Niño+ 1 year. *International Journal of Climatology*, **22 (1)**, 87–106, doi:10.1002/joc.711.

Chinchilla-Ramírez, G., 2014: Resumen Meteorológico Julio 2014. Boletín Meteorológico Mensual. Instituto Meteorológico Nacional, San José, Costa Rica, 1–42 pp.

Cook, K. H. and E. K. Vizy, 2010: Hydrodynamics of the Caribbean Low-Level Jet and Its Relationship to Precipitation. *Journal of Climate*, **23 (6)**, 1477–1494, doi:10.1175/2009JCLI3210.1.

Dai, A. and T. M. L. Wigley, 2000: Global patterns of ENSO-induced precipitation. *Geophysical Research Letters*, **27 (9)**, 1283–1286, doi:10.1029/1999GL011140.

Dee, D. P., et al., 2011: The ERA-Interim reanalysis: configuration and performance of the data assimilation system. *Quarterly Journal of the Royal Meteorological Society*, **137 (656)**, 553–597, doi:10.1002/qj.828.

Delworth, T., S. Manabe, and R. J. Stouffer, 1993: Interdecadal Variations of the Thermohaline Circulation in a Coupled Ocean-Atmosphere Model. *Journal of Climate*, **6 (11)**, 1993–2011, doi:10.1175/1520-0442(1993)006<1993:IVOTTC>2.0.CO;2.

Delworth, T. L. and R. J. Greatbatch, 2000: Multidecadal Thermohaline Circulation Variability Driven by Atmospheric Surface Flux Forcing. *Journal of Climate*, **13 (9)**, 1481–1495, doi:10.1175/1520-0442(2000)013<1481:MTCVDB>2.0.CO;2.

Delworth, T. L. and M. E. Mann, 2000: Observed and simulated multidecadal variability in the Northern Hemisphere. *Climate Dynamics*, **16 (9)**, 661–676, doi:10.1007/s003820000075.

DeWeaver, E. and S. Nigam, 2002: Linearity in ENSO's Atmospheric Response. *Journal of Climate*, **15**, 2446 – 2461.

Donoso, M. and P. Ramírez, 2001: Latin America and the Caribbean: Report on the Climate Outlook Forums for Mesoamerica. In Coping with the climate: A step Forward, Workshop Report: A multi-stakeholder review of Regional Climate Outlook Forums, Pretoria, South Africa, 16 - 20.

Douglas, M. W., 1995: The Summertime Low-Level Jet over the Gulf of California. *Monthly Weather Review*, **123 (8)**, 2334–2347, doi:10.1175/1520-0493(1995)123<2334:TSLLJO>2.0.CO;2.

Douglas, M. W. and J. C. Leal, 2003: Summertime Surges over the Gulf of California: Aspects of Their Climatology, Mean Structure, and Evolution from Radiosonde, NCEP Reanalysis, and Rainfall Data. *Weather and Forecasting*, **18 (1)**, 55–74, doi:10.1175/1520-0434(2003)018<0055:SSOTGO>2.0.CO;2.

Douglas, M. W., A. Valdez-Manzanilla, and R. Cueto, 1998: Diurnal Variation and Horizontal Extent of the Low-Level Jet over the Northern Gulf of California. *Monthly Weather Review*, **126 (7)**, 2017–2025, doi:10.1175/1520-0493(1998)126<2017:DVAHEO>2.0.CO;2.

Durán-Quesada, A. M., 2012: Sources of moisture for Central America and transport based on a Lagrangian approach: variability, contributions to precipitation and transport mechanisms. Ph.D. thesis, Universidade de Vigo.

Durán-Quesada, A. M., L. Gimeno, J. A. Amador, and R. Nieto, 2010: Moisture sources for Central America: Identification of moisture sources using a Lagrangian analysis technique. *Journal of Geophysical Research: Atmospheres*, **115 (D5)**, n/a–n/a, doi:10.1029/2009JD012455.

Enfield, D. B. and E. J. Alfaro, 1999: The Dependence of Caribbean Rainfall on the Interaction of the Tropical Atlantic and Pacific Oceans. *Journal of Climate*, **12 (7)**, 2093–2103, doi:10.1175/1520-0442(1999)012<2093:TDOCRO>2.0.CO;2.

Evans, M. N., M. A. Cane, D. P. Schrag, A. Kaplan, B. K. Linsley, R. Villalba, and G. M. Wellington, 2001: Support for tropically-driven Pacific decadal variability based on paleoproxy evidence. *Geophysical Research Letters*, **28 (19)**, 3689–3692.

Fallas-López, B. and E. J. Alfaro, 2012a: Uso de herramientas estadísticas para la predicción estacional del campo de precipitación en América Central como apoyo a los Foros Climáticos Regionales. 1: Análisis de tablas de contingencia. *Revista de Climatología, 2012, 12: 61-79*.

Fallas-López, B. and E. J. Alfaro, 2012b: Uso de herramientas estadísticas para la predicción estacional del campo de precipitación en América Central como apoyo a los Foros Climáticos Regionales. 2: Análisis de Correlación Canónica. *Revista de Climatología*, **12**.

Feng, L., D. Wu, X. Lin, and X. Meng, 2010: The effect of regional ocean-atmosphere coupling on the long-term variability in the Pacific Ocean. *Advances in Atmospheric Sciences*, **27 (2)**, 393–402, doi:10.1007/s00376-009-8195-3.

Fernández, W., R. Chacón, and Melgarejo, 1996: On the rainfall distribution with altitude over Costa Rica. *Revista Geofísica*, **44**, 57–72.

Fiedler, P. C. and M. F. Lavín, 2006: Introduction: A review of eastern tropical Pacific oceanography. *Progress in Oceanography*, **69 (2-4)**, 94–100, doi:10.1016/j.pocean.2006.03.006.

García-Solera, I. and P. Ramirez, 2012: Central America's Seasonal Climate Outlook Forum. Tech. rep., The Climate Services Partnership, 8 pp.
Gershunov, A. and T. Barnett, 1998a: ENSO influence on intraseasonal extreme rainfall and temperature frequencies in the contiguous United States: Observations and model results. *Journal of Climate*, **11 (7)**, 1575–1586, doi:10.1175/1520-0442(1998)011<1575:EIOIER>2.0.CO;2.
Gershunov, A. and T. Barnett, 1998b: Interdecadal modulation of ENSO teleconnections. *Bulletin of the American Meteorological Society*, **79 (12)**, 2715–2725, doi:10.1175/1520-0477(1998)079<2715:IMOET>2.0.CO;2.
Gershunov, A. and D. R. Cayan, 2003: Heavy Daily Precipitation Frequency over the Contiguous United States: Sources of Climatic Variability and Seasonal Predictability. *Journal of Climate*, **16 (16)**, 2752–2765, doi:10.1175/1520-0442(2003)016<2752:HDPFOT>2.0.CO;2.
Giannini, A., Y. Kushnir, and M. A. Cane, 2000: Interannual Variability of Caribbean Rainfall, ENSO, and the Atlantic Ocean*. *Journal of Climate*, **13 (2)**, 297–311, doi:10.1175/1520-0442(2000)013<0297:IVOCRE>2.0.CO;2.
Gill, A. E., 1980: Some simple solutions for heat-induced tropical circulation. *Quarterly Journal of the Royal Meteorological Society*, **106 (449)**, 447–462, doi:10.1002/qj.49710644905.
Gimeno, L., et al., 2012: Oceanic and terrestrial sources of continental precipitation. *Reviews of Geophysics*, **50 (4)**, n/a–n/a, doi:10.1029/2012RG000389.
Goldenberg, S. B., C. W. Landsea, A. M. Mestas-Nuñez, and W. M. Gray, 2001: The Recent Increase in Atlantic Hurricane Activity: Causes and Implications. *Science*, **293 (5529)**, 474–479, doi:10.1126/science.1060040.
Greatbatch, R. J., 2000: The North Atlantic Oscillation. *Stochastic Environmental Research and Risk Assessment*, **14 (4-5)**, 213–242, doi:10.1007/s004770000047.
Hanstenrath, S., 1991: *Climate Dynamics of the Tropics*. Kluwer Academic Publishers.
Herrera, E., V. Magaña, and E. Caetano, 2015: Air–sea interactions and dynamical processes associated with the midsummer drought. *International Journal of Climatology*, **35**, 1569–1578, doi:10.1002/joc.4077.
Hidalgo, H. G., A. M. Durán-Quesada, J. A. Amador, and E. J. Alfaro, 2015: The Caribbean Low-Level Jet, the Inter-Tropical Convergence Zone and Precipitation Patterns in the Intra-Americas Sea: A Proposed Dynamical Mechanism. *Geografiska Annaler: Series A, Physical Geography*, **97 (1)**, 41–59, doi:10.1111/geoa.12085.
Higgins, R. W., Y. Yao, and X. L. Wang, 1997: Influence of the North American Monsoon System on the U.S. Summer Precipitation Regime. *Journal of Climate*, **10 (10)**, 2600–2622, doi:10.1175/1520-0442(1997)010<2600:IOTNAM>2.0.CO;2.
Higgins, R. W., et al., 2003: Progress in Pan American CLIVAR Research: The North American Monsoon System. *Atmósfera*, **16 (1)**.
Hoerling, M., A. Kumar, and M. Zhong, 1997: El Niño, La Niña, and the nonlinearity of their teleconnections. *Journal of Climate*, **10 (8)**, 1769–1786, doi:10.1175/1520-0442(1997)010<1769:ENOLNA>2.0.CO;2.
Hurrell, J. W., 1996: Influence of variations in extratropical wintertime teleconnections on northern hemisphere temperature. *Geophysical Research*

Letters, **23 (6)**, 665–668, doi:10.1029/96GL00459.
Janowiak, J. E., A. Gruber, C. R. Kondragunta, R. E. Livezey, and G. J. Huffman, 1998: A Comparison of the NCEP–NCAR Reanalysis Precipitation and the GPCP Rain Gauge–Satellite Combined Dataset with Observational Error Considerations. *Journal of Climate*, **11 (11)**, 2960–2979, doi:10.1175/1520-0442(1998)011<2960:ACOTNN>2.0.CO;2.
Kalnay, E., et al., 1996: The NCEP/NCAR 40-Year Reanalysis Project. *Bull. Amer. Meteor. Soc.*, **77 (3)**, 437–471, doi:10.1175/1520-0477(1996)077<0437:TNYRP>2.0.CO;2.
Karnauskas, K. B., R. Seager, A. Giannini, and A. J. Busalacchi, 2013: A simple mechanism for the climatological midsummer drought along the Pacific coast of Central America. *Atmósfera*, **26 (2)**, 261–281, doi:10.1016/S0187-6236(13)71075-0.
Kerr, R. A., 2000: A North Atlantic Climate Pacemaker for the Centuries. *Science*, **288 (5473)**, 1984–1985, doi:DOI:10.1126/science.288.5473.1984.
Knaff, J., 1997: Implications of Summertime Sea Level Pressure Anomalies in the Tropical Atlantic Region. *Journal of Climate*, **10 (4)**, 789 – 804, doi:10.1175/1520-0442(1997)010<0789:IOSSLP>2.0.CO;2.
Latif, M., et al., 2004: Reconstructing, Monitoring, and Predicting Multidecadal-Scale Changes in the North Atlantic Thermohaline Circulation with Sea Surface Temperature. *Journal of Climate*, **17 (7)**, 1605–1614, doi:10.1175/1520-0442(2004)017<1605:RMAPMC>2.0.CO;2.
Lindzen, R. S. and S. Nigam, 1987: On the Role of Sea Surface Temperature Gradients in Forcing Low-Level Winds and Convergence in the Tropics. *Journal of the Atmospheric Sciences*, **44 (17)**, 2418–2436, doi:10.1175/1520-0469(1987)044<2418:OTROSS>2.0.CO;2.
Magaña, V., J. A. Amador, and S. Medina, 1999: The Midsummer Drought over Mexico and Central America. *Journal of Climate*, **12 (6)**, 1577–1588, doi:10.1175/1520-0442(1999)012<1577:TMDOMA>2.0.CO;2.
Maldonado, T. and E. Alfaro, 2010a: Comparación de las salidas del modelo MM5v3 con datos observados en la Isla del Coco, Costa Rica. *Tecnología en Marcha*, **23 (4)**, 3–28.
Maldonado, T. and E. Alfaro, 2010b: Propuesta metodológica para la predicción climática estacional de eventos extremos y días con precipitación. Estudio de caso: Sur de América Central. *InterSedes*, **11 (21)**, 182–214.
Maldonado, T. and E. Alfaro, 2011: Predicción estacional para ASO de eventos extremos y días con precipitación sobre las vertientes Pacífico y Caribe de América Central, utilizando análisis de correlación canónica. *InterSedes*, **12 (24)**, 78–108.
Malmgren, B. A., A. Winter, and D. Chen, 1998: El Niño–Southern Oscillation and North Atlantic Oscillation Control of Climate in Puerto Rico. *Journal of Climate*, **11 (10)**, 2713–2717, doi:10.1175/1520-0442(1998)011<2713:ENOSOA>2.0.CO;2.
Mantua, N. J. and S. R. Hare, 2002: The Pacific Decadal Oscillation. *Journal of Oceanography*, **58 (1)**, 35–44, doi:10.1023/A:1015820616384.
Mantua, N. J., S. R. Hare, Y. Zhang, J. M. Wallace, and R. C. Francis, 1997: A Pacific Interdecadal Climate Oscillation with Impacts on Salmon Production. *Bull. Amer. Meteor. Soc.*, **78 (6)**, 1069–1079,

doi:10.1175/1520-0477(1997)078<1069:APICOW>2.0.CO;2.
Martin, E. R. and C. Schumacher, 2011: Modulation of Caribbean Precipitation by the Madden–Julian Oscillation. *Journal of Climate*, **24 (3)**, 813–824, doi:10.1175/2010JCLI3773.1.
Mestas-Nuñez, A. M. and D. B. Enfield, 2001: Eastern equatorial Pacific SST variability: ENSO and non-ENSO components and their climatic associations. *Journal of Climate*, **14 (3)**, 391–402.
Mock, C. J., 1996: Climatic controls and spatial variations of precipitation in the western United States. *Journal of Climate*, **9 (5)**, 1111–1125.
Molinari, J., D. Knight, M. Dickinson, D. Vollaro, and S. Skubis, 1997: Potential Vorticity, Easterly Waves, and Eastern Pacific Tropical Cyclogenesis. *Monthly Weather Review*, **125 (10)**, 2699–2708, doi:10.1175/1520-0493(1997)125<2699:PVEWAE>2.0.CO;2.
Muñoz, A. G., et al., 2012: Risk management at the latin american observatory, risk management-current issues and challenges. 533 – 556.
Muñoz, E., A. J. Busalacchi, S. Nigam, and A. Ruiz-Barradas, 2008: Winter and Summer Structure of the Caribbean Low-Level Jet. *Journal of Climate*, **21 (6)**, 1260–1276, doi:10.1175/2007JCLI1855.1.
Muñoz, E., C. Wang, and D. Enfield, 2010: The Intra-Americas Sea springtime surface temperature anomaly dipole as fingerprint of remote influence. *Journal of Climate*, **23**, 43–56, doi:http://dx.doi.org/10.1175/2009JCLI3006.1.
Neri, C. and V. Magaña, 2016: Estimation of vulnerability and risk to meteorological drought in Mexico. *Weather, Climate and Society*, **8**.
Oglesby, R., et al., 2016: A High-Resolution Modeling Strategy to Assess Impacts of Climate Change for Mesoamerica and the Caribbean. *American Journal of Climate Change*, **05 (02)**, 202–228, doi:10.4236/ajcc.2016.52019.
Peña, M. and M. W. Douglas, 2002: Characteristics of Wet and Dry Spells over the Pacific Side of Central America during the Rainy Season. *Monthly Weather Review*, **130**, 3054 – 3073.
Poleo, D., E. Solano, and W. Stolz, 2014a: La Oscilación Atmosférica Madden-Julian y las lluvias en Costa Rica. *Tópicos Meteorológicos y Oceanográficos*, **13**, 5 – 18.
Poleo, D., E. Solano, and W. Stolz, 2014b: La Oscilación Madden-Julian y las precipitationes extremas en Costa Rica. *Tópicos Meteorológicos y Oceanográficos*, **13**, 5 – 18.
Poveda, G. and O. J. Mesa, 2000: On the existence of Lloró (the rainiest locality on earth): Enhanced ocean-land-atmosphere interaction by a low-level jet. *Geophysical Research Letters*, **27 (11)**, 1675–1678, doi:10.1029/1999GL006091.
Ramírez, P., 1983: Estudio Meteorológico de los Veranillos en Costa Rica. Nota de investigación. 5, Instituto Meteorológico Nacional, Ministerio de Agricultura y Ganadería., San José, Costa Rica.
Ranjha, R., G. Svensson, M. Tjernström, and A. Semedo, 2013: Global distribution and seasonal variability of coastal low-level jets derived from ERA-Interim reanalysis. *Tellus A*, **65 (0)**, doi:10.3402/tellusa.v65i0.20412.
Retana, J. A., 2012: Eventos hidrometeorlgícos extremos lluviosos en costa rica desde la perspectiva de la adaptación al cambio en el clima. *Ambientales*, **44**, 5 – 16.

Schneider, N. and B. D. Cornuelle, 2005: The Forcing of the Pacific Decadal Oscillation*. *Journal of Climate*, **18 (21)**, 4355–4373, doi:10.1175/JCLI3527.1.
Schneider, U., A. Becker, P. Finger, A. Meyer-Christoffer, B. Rudolf, and M. Ziese, 2011: GPCC Full Data Reanalysis Version 6.0 at 0.5°: Monthly Land-Surface Precipitation from Rain-Gauges built on GTS-based and Historic Data. Tech. rep., Global Precipitation Climatology Centre. doi:10.5676/DWD_GPCC/FD_M_V7_050.
Schultz, D. M., W. E. Bracken, and L. F. Bosart, 1998: Planetary- and Synoptic-Scale Signatures Associated with Central American Cold Surges. *Monthly Weather Review*, **126 (1)**, 5–27, doi:10.1175/1520-0493(1998)126<0005:PASSSA>2.0.CO;2.
Schultz, D. M., W. E. Bracken, L. F. Bosart, G. J. Hakim, M. A. Bedrick, M. J. Dickinson, and K. R. Tyle, 1997: The 1993 Superstorm Cold Surge: Frontal Structure, Gap Flow, and Tropical Impact. *Monthly Weather Review*, **125 (1)**, 5–39, doi:10.1175/1520-0493(1997)125<0005:TSCSFS>2.0.CO;2.
Smith, T., R. Reynolds, T. C. Peterson, and J. Lawrimore, 2007: Improvements to NOAA's Historical Merged Land–Ocean Surface Temperature Analysis (1880–2006). *Journal of Climate*, **21**, 2283 – 2296.
Srinivasan, J. and G. L. Smith, 1996: Meridional Migration of Tropical Convergence Zones. *Journal of Applied Meteorology*, **35 (8)**, 1189–1202, doi:10.1175/1520-0450(1996)035<1189:MMOTCZ>2.0.CO;2.
Taylor, M. A. and E. J. Alfaro, 2005: Climate of Central America and the Caribbean. *Encyclopedia of World Climatology*, J. E. Oliver, Ed., Springer, Netherlands, 183–186.
Trenberth, K. E., 1997: The Definition of El Niño. *Bulletin of the American Meteorological Society*, **78 (12)**, 2771–2777, doi:10.1175/1520-0477(1997)078<2771:TDOENO>2.0.CO;2.
Uribe-Alcántara, E. M., 2002: El inicio de la temporada de lluvias en la costa sudoeste de méxico: Relaciones para su diagnóstico y pronóstico.
Velásquez, R., 2000: Mecanismos físicos de variabilidad climática y eventos extremos en Venezuela. Lic. thesis, Departamento de Física Atmosférica, Oceánica y Planetaria, Escuela de Física, Universidad de Costa Rica.
Vera, C., et al., 2006: Toward a unified view of the American monsoon systems. *Journal of Climate*, **19 (20)**, 4977–5000.
Wahlstrom, M., 2014: Informe regional del estado de la vulnerabilidad y riesgos de desastres en Centroamérica. Tech. rep., CEPREDENAC-UNISDR, 198 pp., Panamá.
Wang, C., 2007: Variability of the Caribbean Low-Level Jet and its relations to climate. *Clim Dyn*, **29 (4)**, 411–422, doi:10.1007/s00382-007-0243-z.
Wang, C. and D. B. Enfield, 2001: The Tropical Western Hemisphere Warm Pool. *Geophysical Research Letters*, **28 (8)**, 1635–1638, doi:10.1029/2000GL011763.
Wang, C. and D. B. Enfield, 2003: A Further Study of the Tropical Western Hemisphere Warm Pool. *Journal of Climate*, **16 (10)**, 1476–1493, doi:10.1175/1520-0442(2003)016<1476:AFSOTT>2.0.CO;2.
Wang, C. and P. C. Fiedler, 2006: ENSO variability and the eastern tropical Pacific: A review. *Progress in Oceanography*, **69 (2–4)**, 239–266, doi:10.1016/j.pocean.2006.03.004.

Wang, C. and S.-k. Lee, 2007: Atlantic warm pool, Caribbean low-level jet, and their potential impact on Atlantic hurricanes. *Geophysical Research Letters*, **34 (2)**, 1–5, doi:10.1029/2006GL028579.

Wang, C., S.-k. Lee, and D. B. Enfield, 2007: Impact of the Atlantic Warm Pool on the Summer Climate of the Western Hemisphere. *Journal of Climate*, **20 (20)**, 5021–5040, doi:10.1175/JCLI4304.1.

Wang, C., S.-K. Lee, and D. B. Enfield, 2008: Climate Response to Anomalously Large and Small Atlantic Warm Pools during the Summer. *Journal of Climate*, **21 (11)**, 2437–2450, doi:10.1175/2007JCLI2029.1.

Warner, T. T., B. E. Mapes, and M. Xu, 2003: Diurnal Patterns of Rainfall in Northwestern South America. Part II: Model Simulations. *Monthly Weather Review*, **131 (5)**, 813–829, doi:10.1175/1520-0493(2003)131<0813:DPORIN>2.0.CO;2.

Wilks, D. S., 2011: *Statistical Methods in the Atmospheric Sciences, Volume 100, Third Edition*. 3d ed., Academic Press, Amsterdam ; Boston.

Xue, Y., T. Smith, and R. Reynolds, 2003: Interdecadal changes of 30-yr SST normals during 1871-2000. *JOURNAL OF CLIMATE*, **16 (10)**, 1601–1612, doi:10.1175/1520-0442-16.10.1601.

Zárate-Hernández, E., 2013: Climatología de masas invernales de aire frío que alcanzan Centroamérica y el Caribe y su relación con algunos índices árticos. *Tópicos Meteorológicos y Oceanográficos*, **12 (1)**, 35 – 55.

Zhang, R. and T. L. Delworth, 2006: Impact of Atlantic multidecadal oscillations on India/Sahel rainfall and Atlantic hurricanes. *Geophysical Research Letters*, **33 (17)**, n/a–n/a, doi:10.1029/2006GL026267.

Zhang, Y., J. M. Wallace, and D. S. Battisti, 1997: ENSO-like interdecadal variability: 1900-93. *Journal of Climate*, **10 (5)**, 1004–1020.

Acronyms

AMO Atlantic Multi-Decadal Oscillation. 12, 20, 22
ASO August-September October. 41, 48, 50, 51, 54, 55
AWP Atlantic Warm Pool. 22

CARCOF Central American Regional Climate Outlook Forum. 48
CCA Canonical Correlation Analysis. vii, 12, 27, 30–32, 35, 39–43, 48, 52, 54–56
CJ Chocó Jet. 16, 18, 21
CLLJ Caribbean Low-Level Jet. vii, 11, 15, 16, 18, 21–24, 33, 35–37, 39, 40, 46, 47, 52, 54, 56
CNDS Centre for Natural Disaster Science. 9
CPC Climate Prediction Center. 27, 29
CS Caribbean Source. 17, 18

ECMWF European Centre for Medium-Range Weather Forecast. 33
ENSO El Niño Southern Oscillation. vii, 11, 12, 20–23, 25, 27, 29, 30, 36, 37, 47, 48, 52–54, 56
ERSST Extended Reconstructed Sea Surface Temperatures. 27
ETPac Eastern Tropical Pacifc. 14–16, 19

FRD Frequency of Rainy Days. 32

GCM General Circulation Model. 9
GPCC Global Precipitation Climatology Centre. 27

IAS Intra-Americas Seas. 14, 16, 20, 22
IFS Integrated Forecast System. 33
ITCZ Intertropical Convergence Zone. 14, 15, 17–20, 23, 24, 29, 45

MJ May-June. 32, 45
MSD Mid-Summer Drough. vii, 11, 12, 14, 19, 23, 24, 26, 27, 29–32, 35, 39–43, 46, 48, 52–54

NAMS North American Monsoon System. 15, 16
NAO North Atlantic Oscillation. 11, 20, 22
NASH North Atlantic Subtropical High. 14, 18, 22, 46
NCEP-NCAR National Centers for Environmental Prediction – National Center for Atmospheric Research. 26

ONI Oceanic El Niño Index. 27, 30

p20 20^{th} percentile. 32
p80 80^{th} percentile. 32, 42
PCA Principal Component Analysis. 31
PDO Pacific Decadal Oscillation. vii, 11–13, 20–22, 26, 29, 30, 35–39, 52, 53, 56
PS Pacific Source. 17, 18

SAMS South American Monsoon System. 15
SLP Sea Level Pressure. 15, 20, 22, 26, 32, 35, 36, 42, 44, 46, 47, 52
SLPA Sea Level Pressure Anomalies. 35–37, 53
SST Sea Surface Temperature. vii, 12, 14, 15, 19–24, 27, 28, 31–35, 38–42, 44–46, 48, 52–56
SSTA Sea Surface Temperature Anomalies. 31, 40, 41, 48, 50, 54

TNA Tropical North Atlantic. 32, 35, 42, 44, 45, 48, 54, 55
TP Total Precipitation. 32, 50
TUTT Tropical Upper Tropospheric Trough. 42, 54

WHWP Western Hemisphere Warm Pool. 14, 20, 22, 23

Acta Universitatis Upsaliensis

Digital Comprehensive Summaries of Uppsala Dissertations from the Faculty of Science and Technology 1438

Editor: The Dean of the Faculty of Science and Technology

A doctoral dissertation from the Faculty of Science and Technology, Uppsala University, is usually a summary of a number of papers. A few copies of the complete dissertation are kept at major Swedish research libraries, while the summary alone is distributed internationally through the series Digital Comprehensive Summaries of Uppsala Dissertations from the Faculty of Science and Technology. (Prior to January, 2005, the series was published under the title "Comprehensive Summaries of Uppsala Dissertations from the Faculty of Science and Technology".)

Distribution: publications.uu.se
urn:nbn:se:uu:diva-304656

ACTA
UNIVERSITATIS
UPSALIENSIS
UPPSALA
2016